The Journal of Neuroscience, July 1992, 12(7): 2765–2784

Nicotine Binding and Nicotinic Receptor Subunit RNA after Chronic Nicotine Treatment

Michael J. Marks,[1] James R. Pauly,[1] Stefan D. Gross,[1] Evan S. Deneris,[3,a] Irm Hermans-Borgmeyer,[3,b] Stephen F. Heinemann,[3] and Allan C. Collins[1,2]

[1]Institute for Behavioral Genetics and [2]Department of Psychology, University of Colorado, Boulder, Colorado 80309 and [3]Molecular Neurobiology Laboratory, The Salk Institute, La Jolla, California 92037

DBA mice were chronically treated with nicotine by continuous intravenous infusion of 4.0 mg/kg/hr for 10 d. Drug-treated mice were tolerant to the acute effects of nicotine on locomotor activity and body temperature. The effect of chronic treatment on the amount of L-^{3}H-nicotine binding and RNA encoding for α_4, the most widely expressed nicotinic α-subunit, was measured in three brain regions. Chronic treatment increased L-^{3}H-nicotine binding in cortex and midbrain but had no effect in cerebellum. In contrast, chronic treatment had no effect on the levels of mRNA encoding for α_4 in any of the three brain regions. Subsequently brains were sectioned and L-^{3}H-nicotine binding was measured using quantitative autoradiographic methods. In addition, the relative amounts of mRNA for the major nicotinic receptor subunits (α_4 and β_2), as well as for three additional minor subunits (α_2, α_3, and α_5), were determined by *in situ* hybridization histochemistry followed by quantitation of image intensity. Chronic nicotine treatment resulted in increases in the amount of L-^{3}H-nicotine binding in many but not all brain areas measured. In contrast, chronic treatment had little effect on the intensity of the hybridization signal for the nicotinic subunit mRNA. The results suggest that chronic treatment with nicotine under conditions resulting in maximal steady-state increases in L-^{3}H-nicotine binding has little effect on RNA levels encoding any of four nicotinic α-subunits and the β_2-subunit.

The continued use of tobacco products results in the development of many signs of tolerance (Surgeon General, 1988). The physiological and biochemical changes that underlie the development of tolerance to nicotine, the principle active component of tobacco, are not fully understood. However, chronic exposure to nicotine results in an increase in the density of binding sites for putative nicotinic receptors in the brains of mice (Marks et al., 1983), rats (Schwartz and Kellar, 1983), and humans (Benwell et al., 1988). Studies from our laboratory using the DBA/2 mouse strain have shown that the sites labeled with L-^{3}H-nicotine increase with treatment time (Marks et al., 1985) and treatment dosage (Marks et al., 1983, 1986a) and decrease to control levels following withdrawal (Marks et al., 1985) in patterns closely approximating the changes in sensitivity to nicotine.

Characterization of putative nicotinic receptors in brain using receptor binding techniques indicates that at least two major classes of binding sites exist: one labeled by high-affinity binding of L-^{3}H-nicotine or ^{3}H-ACh and a second labeled with α-^{125}I-bungarotoxin (Clarke et al., 1985; Marks et al., 1986b). The application of molecular techniques to the study of brain nicotinic receptors has demonstrated that the heterogeneity of these receptors is much greater than indicated by binding studies. The nicotinic receptor in brain seems to be composed of only two types of subunit, α and β (for review, see Luetje et al., 1990). Four α-subunits and three β-subunits have been identified in rat brain, to date (Boulter et al., 1986, 1990; Goldman et al., 1987; Deneris et al., 1988, 1989; Wada et al., 1988; Duvoisin et al., 1989). As is the case with the muscle receptors, the α-subunits interact with agonists such as ACh or nicotine. The distribution of RNA encoding for several of these subunits in brain indicates that each one has a unique localization (Goldman et al., 1987; Deneris et al., 1989; Duvoisin et al., 1989; Wada et al., 1989; Boulter et al., 1990). Functional ion channels have been reconstituted using *Xenopus* oocytes, in which the combination of *in vitro* transcripts of one α (α_2, α_3, or α_4) with those of a single β (β_2 or β_4) results in the expression of agonist-sensitive ion channels (Boulter et al., 1987; Duvoisin et al., 1989; Papke et al., 1989). Characterization of α-bungarotoxin binding components in the CNS has also begun, and two related α-subunits have been identified in chick brain (Couturier et al., 1990; Schoepfer et al., 1990).

One receptor subtype (α_4, β_2) appears to account for most (>90%) of the nicotine binding in rat brain (Whiting and Lindstrom, 1986; Whiting et al., 1987; Lindstrom et al., 1990), and a cell line transfected with chick α_4 and β_2 genes expresses high-affinity nicotine binding (Whiting et al., 1991). In addition, the similarity in the distribution of L-^{3}H-nicotine binding sites (Clarke et al., 1985) and of sites labeled with monoclonal antibody (MAb) 270, which recognizes the β_2-subunit of nicotinic ACh receptors (Swanson et al., 1987), is consistent with that assignment of the β_2-subunit as the primary structural subunit. Fur-

Received Sept. 27, 1991; revised Feb. 12, 1992; accepted Feb. 18, 1992.

This research was supported by Grants DA-03194 and DA-00116 from NIDA and Grants AA-08388 and AA-06391 from NIAAA to the authors in Boulder and NIH Jacob Javits Investigator Award from NIH, Tobacco-Related Disease Research Program, University of California, and MDA research grant to Dr. Heinemann. We thank Dr. Scott Rogers for helpful comments on the manuscript, Dr. Jim Boulter for useful discussions, and Mike Adler for supplying the α_5-construct.

Correspondence should be addressed to Michael Marks, Institute for Behavioral Genetics, Campus Box 447, University of Colorado, Boulder, CO 80309.

[a] Present address: Department of Neuroscience, School of Medicine, Case-Western Reserve University, Cleveland, OH 44106.

[b] Present address: ZMNH-II, Universitat Hamburg, Hamburg, Germany.

thermore, the distribution of RNA encoding both the α_4- and β_2-subunits of the nicotinic ACh receptor in rat brain is similar to the distribution of both L-^{3}H-nicotine and MAb 270 binding sites. The correspondence is not perfect, however, suggesting that some L-^{3}H-nicotine binding sites encoded by α_4 are presynaptic or that some L-^{3}H-nicotine binding sites may be encoded by other α-genes. It is also possible that the subunits coded by the other members of this complex gene family are not detected by L-^{3}H-nicotine. Clearly, the receptors encoded by the other genes may be important in influencing responsiveness to nicotine, and changes in these receptors after nicotine treatment may be important in modulating tolerance to the effects of nicotine.

The present study was undertaken to investigate whether the changes in L-^{3}H-nicotine binding sites observed in mice after chronic exposure to nicotine may be due to changes in the levels of mRNA for four α-subunits and the major β-subunit that encode the protein subunits of the nicotinic ACh receptor in brain.

Materials and Methods

Materials. Uridine triphosphate (α-^{35}S) and uridine triphosphate (α-^{32}P) were obtained from New England Nuclear (Boston, MA). L-Nicotine (methyl-^{3}H) and Hyperfilm-^{3}H were obtained from Amersham Corp. (Arlington Heights, IL). Adenosine triphosphate, cytosine triphosphate, guanosine triphosphate, and RNase A were purchased from Boehringer-Mannheim (Indianapolis, IN). The enzymes EcoRI, HindIII, SP6 RNA polymerase, T3 RNA polymerase, and RQ1 DNase, as well as the RNasin, were obtained from Promega Corp. (Madison, WI). Dextran sulfate was purchased from Pharmacia (Uppsala, Sweden) and formamide from Fluka Chemical Corp. (Ronkonkoma, NY). DPX mountant was purchased from BDH Ltd. (Poole, England). Ammonium acetate, morpholine propane sulfonic acid, Tris, Tris hydrochloride, 1-piperazincdiethanesulfonic acid (PIPES), sodium carbonate, sodium bicarbonate, gelatin, RNase T1, yeast tRNA, total yeast RNA, triethanolamine, sodium chloride, sodium citrate, phenol, magnesium chloride, dithiothreitol (DTT), disodium EDTA, Denhardt's solution, acetic anhydride, poly-L-lysine, diethylpyrocarbonate, sodium hydroxide, trichloroacetic acid (TCA), guanidinium thiocyanate, and sodium phosphate were obtained from Sigma Chemical Co. (St. Louis, MO). Microscope slides and coverslips were products of Richard-Allen (Richfield, MI).

Mice. Female DBA/2J/Ibg mice were used in this study. Animals were between 60 and 90 d of age at the time of surgery. Before surgery, the mice were housed five per cage and were allowed free access to food (Wayne Lab Blox) and water. A 12 hr light/12 hr dark cycle was maintained (lights on 7 A.M. to 7 P.M.).

Surgery. A cannula made of Silastic tubing was implanted in the right jugular vein of each mouse using the method of Barr et al. (1979). After surgery, mice were transferred to individual treatment cages and cannulas were attached to polyethylene tubing connected to a syringe mounted on a Harvard infusion pump (Harvard Instruments, South Natick, MA). Continuous infusion with sterile isotonic saline was then begun (flow rate, 35 μl/hr).

Chronic nicotine treatment. After a 2 d recovery period, saline infusion was continued for control mice and nicotine treatment was initiated for drug-treated mice. The final treatment dosage of 4.0 mg/kg/hr was attained by initiating infusion at a rate of 1.0 mg/kg/hr and increasing the dosage by 1.0 mg/kg/hr per day until the final infusion rate was achieved. Mice were maintained at the 4.0 mg/kg/hr dose for a total of 10 d.

Measurement of acute responsiveness to nicotine. On the tenth day of treatment with 4.0 mg/kg/hr nicotine (thirteenth day of drug treatment), each mouse was tested for sensitivity to nicotine. Two hours after cessation of treatment, saline was injected intraperitoneally and activity in a Y-maze and body temperature were measured. Two hours after completion of the baseline measurement, each mouse was injected intraperitoneally with 1.0 mg/kg nicotine and activity and temperature were measured again. Injection vehicle was sterile isotonic saline, and the injection volume was 0.01 ml/gm. The Y-maze test was conducted for 3 min beginning 5 min after injection of either saline or nicotine. Body temperature was measured 15 min after injection using a Thermalert rectal thermometer (Bailey Instruments, Saddlebrook, NJ). The Y-maze and body temperature tests were used to evaluate responsiveness to nicotine because these measures have provided reliable estimates of initial sensitivity to nicotine (Marks et al., 1989) and tolerance development (Marks et al., 1986a). Preliminary studies with untreated animals indicated that measurement of responses of a mouse twice in a day (one saline and one nicotine test) gave results virtually identical to those obtained using animals tested only with nicotine or with saline. The double testing of the mice allowed measurement of responses after acute injection of saline and nicotine in each mouse.

At the completion of the tolerance tests, mice were returned to their treatment cages and infusion was continued.

Tissue preparation. The day following the tolerance tests, each mouse was removed from its infusion cage and its cannula was checked for free flow. The mouse was then killed by cervical dislocation, and its brain was rapidly removed and frozen by immersion in isopentane (−35°C) and stored at −70°C until sectioning.

Brains were sectioned using an IEC cryostatic microtome (International Equipment Corp., Needham Heights, MA) refrigerated to −16°C. Coronal sections 14 μm thick were thaw mounted onto 25 mm × 75 mm glass microscope slides that had been treated both with gelatin/chrome alum and poly-L-lysine (Simmons et al., 1989). Nine sets of serial sections (approximately 80 sections per set) were collected from each mouse so that ligand binding and *in situ* hybridizations could be performed for each mouse. At the completion of the sectioning, slides were dried under vacuum and stored, dessicated, at −70°C until use.

Nicotine binding for quantitative autoradiography. One set of sections was used to measure the binding of L-^{3}H-nicotine. The experimental procedures were similar to those reported by Pauly et al. (1989). Briefly, sets of 25 slides were incubated in 200 ml of Krebs–Ringers HEPES (NaCl, 118 mM; KCl, 4.8 mM; $CaCl_2$, 2.5 mM; $MgSO_4$, 1.2 mM; HEPES, 20 mM; pH to 7.5 with NaOH) for 30 min at 4°C to rinse the tissue and remove endogenous ACh and/or nicotine remaining from the treatment. The slides were then transferred to 200 ml of Krebs–Ringers HEPES containing 5.1 nM L-^{3}H-nicotine (Amersham, Arlington Heights, IL; specific activity, 68.0 Ci/mmol) and incubated for 90 min at 4°C. After the incubation with the radiolabeled nicotine, the slides were washed as follows: Krebs–Ringers HEPES, 2 × 5 sec; 20 mM HEPES (pH 7.5), 2 × 5 sec; and water, 2 × 5 sec. Wash temperature was 4°C. The slides were then air dried at room temperature and apposed to Hyperfilm-^{3}H for 6 weeks. Subsequently, 4 week and 8 week exposure times were used to assure that film response was not saturated for areas that bound large amounts of nicotine and to allow sufficient exposure time for areas that bound relatively little nicotine.

Incubation and wash conditions were established from preliminary experiments in which ligand binding was monitored by scintillation counting of counts bound to tissue scraped from slides. The conditions are very similar to those employed in the measurement of binding to tissue homogenates (Marks et al., 1986b). Binding in the presence of 10 μM unlabeled nicotine did not exceed film background.

In situ *RNA hybridization.* The method for *in situ* hybridization using riboprobes is identical to that described by Wada et al. (1989) and Simmons et al. (1989), with the exception that the tissue was fixed *in vitro,* rather than by perfusion *in vivo.*

Probes were prepared using *in vitro* transcription and α-^{35}S-UTP as the sole source of UTP. The constructs used to synthesize the probes were α_2: clone HYP16(REV) (HYP16 subcloned in pSP64 in antisense orientation relative to the SP6 promoter), linearized with HindIII, synthesized using SP6 RNA polymerase; α_3: clone pPCA48E(4), cloned in pSP65, linearized with HindIII, synthesized using SP6 RNA polymerase; α_4: clone pHYA23-1E(2), cloned in pSP64, linearized with EcoRI, synthesized using SP6 RNA polymerase; α_5: clone PC989 subcloned into pBluescript (generously supplied by M. Adler), linearized with EcoRI, synthesized using T3 RNA polymerase; and β_2: clone pSP65-49, cloned in pSP65, linearized with HindIII, synthesized using SP6 RNA polymerase. Each synthesis was designed to yield full-length antisense transcripts. Products were analyzed by electrophoresis through denaturing agarose gels. The cRNAs were stored as precipitates in 70% ethanol at −20°C until use. Hybridizations were performed within 3 d of probe synthesis. Immediately before hybridization, probes were subjected to alkaline hydrolysis using the method of Cox et al. (1984) to yield products with average sizes of 500 bases.

On the day of the hybridizations, slides containing tissue sections were removed from the freezer, warmed to room temperature under vacuum, incubated for 15 min with 4% paraformaldehyde in PBS (phosphate-buffered saline: NaCl, 137 mM; KCl, 2.5 mM; Na_2HPO_4, 16 mM; and NaH_2PO_4, 4 mM; pH 7.4) to fix the tissue. After fixation, the slides were washed three times for 5 min each in PBS and followed by air drying. After drying, tissue sections were acetylated by incubation for 10 min with 15 mM acetic anhydride in 0.1 M triethanolamine, pH 8.0. Slides were then rinsed for 2 min in 2× SSC (1× SSC: NaCl, 150 mM; trisodium citrate, 15 mM; pH to 7.0 with HCl) and dehydrated by passage through an ethanol series (3 min each: 50%, 70%, 95%, 100%, and 100%). After dehydration, the slides were air dried and then stored under vacuum until the hybridization was begun (storage time, 2–4 hr).

^{35}S-radiolabeled cRNA probes, prepared as described above, were dissolved in hybridization buffer (formamide, 50%; dextran sulfate, 10%; NaCl, 300 mM; Tris, 10 mM; EDTA, 1 mM; yeast tRNA, 500 μg/ml; DTT, 10 mM; 1× Denhardt's solution; pH 8.0) to a final concentration of 5×10^6 cpm/ml. Hybridizations were begun by applying 100 μl of hybridization solution to a 24 mm × 60 mm glass coverslip and then placing the slide containing the sections over the coverslip. The edges of the coverslip were sealed with DPX, and the samples were incubated in a 58°C oven for 18 hr.

After the 18 hr incubation, the DPX was peeled off and the coverslips removed by agitation for 15 min in 4× SSC. The slides were then washed four more times (5 min each) with 4× SSC and subsequently transferred to a ribonuclease-containing buffer [RNase A, 20 μg/ml; NaCl, 500 mM; Tris (pH 8.0), 10 mM; EDTA, 1 mM] and incubated at 37°C for 30 min to digest nonhybridized, single-stranded RNA. The slides were then washed and gradually desalted by incubation for 5 min each in 2× SSC, 2× SSC, 2× SSC, 1× SSC, and 0.5× SSC. All these SSC solutions contained 1 mM DTT to prevent oxidation of the ^{35}S-containing probes. A 30 min high-stringency wash was performed by incubation in 0.1× SSC containing 1 mM DTT at 60°C for 30 min. The slides were then placed in 0.1× SSC containing 1 mM DTT until cool (10 min), and dehydrated by passage through an ethanol series, 3 min each in 50%, 70%, 95%, 100%, 100%, and 100%. Slides were then air dried and exposed to Amersham Hyperfilm-^{3}H for 3–10 d.

Optimum hybridization conditions and reproducibility of the hybridizations were determined in the following preliminary experiments. (1) Hybridization as a function of probe length [full length (about 2000 bases), 1000 bases, 500 bases, 250 bases, and 125 bases; optimum signal was obtained with 500 bases]. (2) Hybridization as a function of probe concentration (input radioactivity, 2×10^5, 5×10^5, 1×10^6, 2×10^6, 5×10^6, 1×10^7, and 2×10^7 cpm/ml); hybridization signal increased with each increase in probe concentration, but optimum signal to noise ratio was obtained using 5×10^6 cpm/ml. (3) Hybridization as a function of incubation time (4 hr, 8 hr, 16 hr, 24 hr, and 42 hr); maximum signal was obtained between 16 and 24 hr. (4) Hybridization reproducibility by comparison of signal obtained in four sets of serial sections (average variation for 10 brain areas representing the range of hybridization signals was 10.1%). Percentage errors were comparable regardless of signal intensity. (5) Signal intensity was measured as a function of section thickness using the probe for β_2 to determine whether the hybridization methods used could detect differences in tissue mRNA content. The results indicated that signal intensity increased linearly for sections between 8 μm and 14 μm thick.

Quantitation of films. In order to relate the intensity of the film image to a relative measure of tissue radioactivity, standards containing known amounts of either ^{3}H or ^{35}S were exposed along with tissue on each film. Tissue standards were used for ^{35}S, and both plastic standards and tissue standards were used for ^{3}H. Tissue standards were prepared by mixing measured amounts of isotope with a homogenate prepared from whole brain. Actual concentrations of radioactivity were measured in weighted aliquots. The ^{3}H standards contained from 0 to 4.5 nCi/mg, and the ^{35}S standards contained from 0 to 25 nCi/mg. Eight standards were used for each isotope.

The tissue standards were used to construct standard curves relating both gray level and optical density to radioactivity. These curves were then used to calculate relative radioactive content (cpm/mg) in specific brain areas. Nuclei were identified by overlaying the autoradiograms, and the thionin-stained sections and gray levels were measured using a Drexel University Image Analysis System (DUMAS) and the associated BRAIN software. Hardware used included a Dell 316 microcomputer (Dell Corp., Houston, TX), Circon 9015-H solid-state video camera (Circon Corp., Santa Barbara, CA), Chroma-pro 45 DUMAS light source (Circle S Inc., Tempe, AZ), and a Datacube IVG-128 image processor (Datacube Inc., Peabody, MA). At least 5 and as many as 40 measurements were taken from each region for each animal, and the values thus obtained were averaged to provide the estimate of regional binding or hybridization for that animal. In addition to the quantitation of nuclei that displayed distinct signals above background, at least two brain areas that had no detectable signal were measured to estimate nonspecific hybridization.

t tests were used to compare signal intensity in the control and nicotine-treated groups within each brain nucleus.

The reproducibility of the results was determined by analyzing two sets of sections from control and drug-treated mice that had been hybridized for α_4 mRNA at two different times using independently prepared cRNA probes. The results were subsequently compared using correlational analysis comparing the intensity of hybridization in the first experiment to that obtained in the second for both saline- and nicotine-treated mice. The correlation coefficients between the sets of data obtained in the two experiments were 0.95 and 0.97 for saline-treated and nicotine-treated mice, respectively. This result indicates that the measurement of the relative levels of hybridization was very reproducible. It should be noted that the absolute measurements of hybridization differed between the experiments, suggesting that the values measured provide reliable measurement of relative hybridization, rather than quantitative assessment of mRNA levels.

The limits of detection of differences in signal intensity were also estimated by exposing a series of 11 tissue standards containing ^{35}S to film and quantitating signal intensity. The results indicated that samples differing in isotope content by 12% or less could not be differentiated, while those differing in isotope content by 19% or more could be distinguished.

Solution RNA hybridization. Measurement of α_4 mRNA in solution was accomplished using cRNA probe synthesized from linearized pPHY23-1E(2) using α-^{32}P-UTP (specific activity, 1350 Ci/mmol when used) as the sole source of UTP. Mice that had been infused with either saline or 4.0 mg/kg/hr nicotine were killed by cervical dislocation. Their brains were removed and cerebral cortex, cerebellum, and "midbrain" (thalamus and mesencephalon) were dissected and weighed. RNA was then extracted using the guanidinium thiocyanate/acid phenol method of Chomczynski and Sacchi (1987). RNA concentration was measured by absorbance at 260 nm.

The amount of mRNA for α_4 was estimated using the solution hybridization method described by Lee and Costlow (1987). Hybridization was conducted at 58°C in 20 μl of the following buffer: formamide, 50%; NaCl, 400 mM; PIPES, 25 mM; EDTA, 1 mM; pH 6.8. Three or four concentrations of tissue RNA (5–30 μg) were used for each brain area, and total RNA content was maintained at 100 μg/incubation by varying the amount of total yeast RNA added to the mix. Radiolabeled probe (500,000 cpm) was present in excess. At the completion of the hybridization reaction (16 hr), single-stranded RNA, including nonhybridized probe was digested by incubation with RNase A (65 μg) and RNase T1 (150 U) at 37°C for 1 hr in a final volume of 300 μl (buffer: NaCl, 375 mM; Tris, 75 mM, EDTA, 5 mM; pH 8.0). After RNase treatment, 200 μg of yeast RNA was added as carrier and TCA was added to a final concentration of 5% to precipitate nonhydrolyzed, double-stranded RNA and carrier. After a 10 min incubation on ice, samples were filtered onto GC50 glass fiber filters (Microfiltration Systems, Dublin, CA). Filters were washed six times with ice-cold 5% TCA and placed in vials, 2.5 ml of Budget Solve (RPI, Arlington Heights, IL) was added, and radioactivity was determined using a Beckman 1800 scintillation counter (counting efficiency, 90%). Content of α_4-mRNA per microgram of RNA was estimated as the slope of the regression line relating acid-precipitable counts to amount of tissue extract.

L-^{3}H-nicotine binding to tissue homogenates. The binding of L-^{3}H-nicotine was measured using a modification of the method of Romano and Goldstein (1980) as described previously (Marks and Collins, 1982; Marks et al., 1986b). Mice that had been infused with either saline or 4.0 mg/kg/hr nicotine were killed by cervical dislocation. Their brains were removed and cerebral cortex, cerebellum, and "midbrain" (thalamus and mesencephalon) were dissected and tissue prepared using the method of Romano and Goldstein (1980). A single concentration of radiolabeled nicotine (3.9 ± 0.2 nM) was used for these assays. Specific binding was determined as the difference in binding between samples containing no nonradioactive nicotine and those containing 10 μM unlabeled L-nicotine. Protein was measured using the method of Lowry et al. (1951).

Table 1. Responses of control and treated mice to acute nicotine injection

Chronic treatment	Saline challenge			Nicotine challenge (1.0 mg/kg)		
	Y-Maze crossings	Y-Maze rearings	Body temperature	Y-Maze crossings	Y-Maze rearings	Body temperature
Saline	61.6 ± 4.6	25.6 ± 2.2	38.4 ± 0.1	15.4 ± 5.4	2.8 ± 1.2	34.4 ± 0.5
4.0 mg/kg/hr	57.7 ± 4.1	22.3 ± 2.2	38.2 ± 0.1	61.2 ± 9.1	9.1 ± 2.4	36.8 ± 0.5
t	0.63	1.03	1.00	4.33***	2.39*	3.38***

Y-Maze activity (crosses and rears) and body temperature were measured in saline- and nicotine-treated mice after acute injection of saline or 1.0 mg/kg nicotine. Results shown are mean ± SEM for 12 mice in each group. Groups were compared with *t* tests (*, $p < 0.05$; ***, $p < 0.001$).

Results

Tolerance. The responses of mice chronically treated with saline or nicotine (4.0 mg/kg/hr) to acute challenge doses of saline or 1.0 mg/kg nicotine are summarized in Table 1. Values for Y-maze activity (crosses and rears) and body temperature did not differ between the treatment groups after acute injection of saline. However, mice that had been chronically treated with 4.0 mg/kg/hr nicotine were significantly less responsive to a challenge injection of 1.0 mg/kg nicotine than were saline-treated mice, indicating that tolerance to the effects of nicotine had developed in these animals.

Solution hybridization and ligand binding in homogenates. In order to determine whether chronic nicotine infusion resulted in changes in the amount of L-^{3}H-nicotine binding and/or mRNA for α_4, ligand binding and mRNA levels were measured. The mRNA for α_4 was measured by RNase protection of mRNA/cRNA hybrids in solution. The RNA was extracted from three large brain areas dissected from control and nicotine-treated mice. RNA levels measured in this manner were compared to L-^{3}H-nicotine binding measured in these same areas from different animals. Results of these experiments are summarized in Table 2. Chronic drug infusion resulted in significant increases in the amount of L-^{3}H-nicotine binding in tissue prepared from cerebral cortex and from "midbrain" (representing thalamus and mesencephalon), but chronic treatment had no significant effect on ligand binding in cerebellum. In contrast to the increases observed in the numbers of nicotinic receptors measured with L-^{3}H-nicotine after chronic nicotine infusion, no changes in the amount of mRNA for α_4 measured using solution hybridization were observed in any of the three brain areas (Table 2).

Table 2. Nicotine binding and α_4-cRNA hybridization in brain regions from control and nicotine-treated mice

Brain region	Control	Treated	*t*
L-^{3}H-nicotine bound (fmol/mg protein)			
Cerebellum	8.9 ± 1.1	10.0 ± 0.8	0.81
Cerebral cortex	34.3 ± 3.9	58.1 ± 4.1	4.20***
Midbrain (thalamus and mesencephalon)	90.4 ± 7.8	123.8 ± 9.5	2.71**
Antisense α_4 RNA hybridized (nCi ^{32}P/μg RNA)			
Cerebellum	0.15 ± 0.02	0.16 ± 0.03	0.26
Cerebral cortex	0.48 ± 0.03	0.46 ± 0.02	0.40
Midbrain (thalamus and mesencephalon)	1.07 ± 0.04	1.12 ± 0.05	0.81

Brains from two separate groups of control and nicotine-treated mice were removed and three brain regions dissected. Total particulate protein was prepared from one group for measurement of ^{3}H-nicotine binding, and RNA was extracted from the second group for measurement of α_4-RNA by solution hybridization. Results represent mean ± SEM for both ligand binding ($n = 10$) and solution hybridization ($n = 6$). Results from control and drug-treated mice were compared with *t* tests (**, $p < 0.01$; ***, $p < 0.001$).

Autoradiographic determination of nicotine binding and nicotinic-subunit mRNAs. The experiment described above indicated that chronic treatment with nicotine resulted in increases in L-^{3}H-nicotine binding in two of three brain regions but had no effect on mRNA levels for α_4 in any of the three dissected brain areas. The level of resolution obtained by dissection is small, and therefore, changes that may have occurred in discrete brain areas would not be observed. Subsequently, ligand binding and *in situ* hybridizations were performed on tissue sections and signal intensity was measured densitometrically.

Nicotine binding. Patterns of ligand binding and the effects of chronic nicotine treatment on this binding are illustrated in Figure 1*A–F* for saline-infused mice and in Figure 1*G–L* for nicotine-infused mice. A detailed qualitative description of the distribution of nicotine binding in mouse brain has been presented previously (Pauly et al., 1989). Nicotine binding is widely distributed throughout the brain. Many areas in the telencephalon bind nicotine, but the binding is generally of low to moderate density. In contrast, many regions in the diencephalon show high density of nicotine binding, including many thalamic nuclei, the medial habenula, the ventral lateral and dorsal lateral geniculate nuclei, and the optic tract nucleus. The interpeduncular nucleus in the mesencephalon possesses the highest density of nicotine binding sites in the brain. Several rhombencephalic nuclei demonstrate nicotine binding, but the density of binding to these sites is relatively modest. The cerebellum is virtually devoid of nicotine binding. Quantitative values for ligand binding in 93 brain regions are summarized in Table 3.

The effects of chronic nicotine infusion on the binding of L-^{3}H-nicotine are also summarized in Table 3. The chronic treatment resulted in substantial and widely distributed increases in ligand binding. Statistically significant increases in L-^{3}H-nicotine binding occurred in every major brain area. In the telencephalon every region in neocortex and rhinencephalon displayed significant increases in ligand binding, while in basal ganglia six of seven areas analyzed displayed significant increases. In contrast, just one of three septal areas was significantly increased after nicotine infusion. Ligand binding sites in some diencephalic areas were more resistant to change following chronic drug treatment. Only 7 of 19 thalamic areas analyzed demonstrated significantly increased binding of L-^{3}H-nicotine, while 5 of 8 me-

tathalamic regions showed elevated binding. In contrast, two of three regions in the epithalamus and the subthalamus and all five regions in the hypothalamus were affected by nicotine infusion. Every (17 of 17) mesencephalic region, except the interpeduncular nucleus, responded to chronic nicotine treatment. (In order to determine if the lack of effect occurred because the film was overexposed, image intensity was also determined on films after a short exposure with the same result.) Most areas in the pons (four of five) and the medulla (three of four) responded to chronic nicotine treatment with increased levels of L-^{3}H-nicotine binding. The low density of binding sites in the cerebellum was unaffected by nicotine infusion.

The average variation (SE) in signal intensity was 6.7% of the mean for areas of control mice and 5.7% of the mean for areas of nicotine-treated mice. On average, the signal measured for L-^{3}H-nicotine binding for nicotine-treated mice was 42% higher than that measured for control mice.

In situ *hybridization, α_4.* In order to determine whether the changes in L-^{3}H-nicotine binding that occurred with chronic nicotine infusion resulted from changes in the levels of mRNA for α_4, which encodes most of the receptors measured with L-^{3}H-nicotine (Whiting and Lindstrom, 1986; Whiting et al., 1987; Lindstrom et al., 1990), *in situ* hybridizations were performed using sections nearly adjacent to those used to measure L-^{3}H-nicotine binding. α_4-mRNA was widely distributed, as illustrated in Figure 2*A–F*. Relative quantitative values for α_4-signal are summarized in Table 4. In general, the nuclei that displayed the most intense hybridization were located in the diencephalon and the mesencephalon. Regions in the diencephalon that showed strong signals for α_4 include thalamic areas, the medial habenula, the lateral pretectal area, the medial geniculate, the dorsal lateral geniculate, and the diagonal band of the septum. Many areas of the septum, thalamus, and metathalamus had moderately strong hybridization, as well. The substantia nigra (pars compacta and pars lateralis) had the highest levels of message with values 1.5–2-fold greater than the levels in any other brain regions. Several areas in the mesencephalon had moderate hybridization. Only a few discrete nuclei in the hindbrain displayed detectable α_4 signal: the lateral dorsal pontine nucleus had a relatively strong hybridization signal; the dorsal tegmental nucleus, pontine nuclei, and the locus coeruleus had moderate signals; while the reticular brainstem region had a relatively weak signal.

In general, the intensity of hybridization in the telencephalon was weak to moderate, but a distinct rostrocaudal pattern was observed in cerebral cortex. The hybridization pattern in the cingulate cortex changed from a relatively uniform, modest signal to a distinct laminar pattern during rostrocaudal progression. The signal in the lateral cingulate was twice that in the medial cingulate. The retrosplenial cortex and the lateral orbital cortex had moderate levels of hybridization. The frontal cortex displayed four distinct bands of hybridization: the outermost layers had relatively little hybridization, while the signal in the deepest cortical layers was approximately three times greater. Two distinct layers were observed in the parietal cortex: a superficial layer that was lightly hybridized and a deeper layer with a threefold greater signal. Three layers were visible in the occipital cortex: an outer layer with little or no signal, a modestly labeled middle layer, and a more strongly labeled deeper layer. Except for the subiculum and the presubiculum, which have moderate to strong signals, little hybridization was found in hippocampus. While the claustrum and the endopiriform nucleus of the basal ganglia had relatively high levels of α_4 mRNA, hybridization in the caudate putamen was very low.

The values measured for α_4-hybridization in mice infused with saline or 4.0 mg/kg/hr nicotine are summarized in Table 4. In addition, the effect of nicotine infusion on the hybridization patterns is illustrated in Figure 2 (panels *A–F* for control mice and panels *G–L* for treated mice). None of the values measured in 59 brain areas in drug-treated mice differed from those measured in control animals.

The average variation (SE) in the measurements was 7.4% of the mean for areas of control mice and 7.5% of the mean for areas of nicotine-treated mice. On average, the signal measured for α_4-hybridization for nicotine-treated mice was 0.1% lower than that measured for control mice.

In situ *hybridizations, β_2.* In order to determine whether the changes in L-^{3}H-nicotine binding that occurred with chronic nicotine infusion resulted in changes in the levels of mRNA for β_2, which encodes the structural subunit for most of the receptors measured with L-^{3}H-nicotine (Whiting and Lindstrom, 1986; Whiting et al., 1987; Lindstrom et al., 1990), *in situ* hybridizations were performed with sections nearly adjacent to those used to measure L-^{3}H-nicotine binding and α_4 hybridization. Hybridization of β_2 was very widely distributed, as illustrated in Figure 3*A–F*. Relative quantitative values for β_2 hybridization are summarized in Table 5. Strong signals for β_2 were observed throughout the brain.

The hybridization signal did not vary markedly among the

→

Figure 1. Autoradiograms for L-^{3}H-nicotine binding. Dark-field photographs of autoradiograms of L-^{3}H-nicotine binding are shown at six levels for both saline treatment (*A–F*) and nicotine treatment (*G–L*). Brighter images indicate more intense binding. Abbreviations: *AHA,* anterior hypothalamic area; *BST,* bed n. of stria terminalis; *CB,* cerebellum; *CG,* central gray; *CGL,* cingulate cortex; *CL,* claustrum; *CP,* caudate putamen; *CX1,* cerebral cortex, layer 1; *DG,* dentate gyrus; *DLG,* dorsal LGN; *DT,* dorsal tegmental n.; *EN,* endopiriform n.; *IC,* inferior colliculus; *LC,* locus coeruleus; *LD,* laterodorsal thalamic n.; *LR,* linear raphe; *MG,* medial geniculate; *MH,* medial habenula; *MP,* medial mammillary n., posterior part; *OT,* olfactory tubercule; *PR,* pontine reticular n.; *RE,* reuniens thalamic n.; *RSPL,* retrosplenial cortex; *RT,* reticular thalamic n.; *SNC,* substantia nigra, compact part; *SNR,* substantia nigra, reticular part; *SUB,* subiculum; *VL,* ventrolateral thalamic n.; *VLGM,* ventral LGN, magnocellular part; *VLGP,* ventral LGN, parvocellular part; *VPL,* ventral posterolateral thalamic n.; *VPM,* ventral posteromedial thalamic n.; *ZI,* zona incerta. Note: some differences in signal intensity in these autoradiograms result from differences in the level of sectioning. See Table 3 for quantitative presentation of binding data.

Figure 2. Autoradiograms for *in situ* hybridization to message for α_4. Dark-field photographs of autoradiograms of α_4-cRNA hybridization are shown at six levels for saline treatment (*A–F*) and nicotine treatment (*G–L*). Brighter images indicate more intense hybridization. Abbreviations: *BST,* bed n. of stria terminalis; *CA1,* CA1 field of hippocampus; *CB,* cerebellum; *CGL,* cingulate cortex; *CP,* caudate putamen; *DG,* dentate gyrus; *DK,* n. Darkshewitsch; *DLG,* dorsal lateral geniculate; *DT,* dorsal tegmental n.; *EN,* endopiriform n.; *FR,* fasciculus retroflexus; *IC,* inferior colliculus; *IF,* interfascicular n.; *LC,* locus coeruleus; *LD,* laterodorsal thalamic n.; *MD,* mediodorsal thalamic n.; *MG,* medial geniculate; *MH,* medial habenula; *OT,* olfactory tubercle; *RSPL,* retrosplenial cortex; *SN,* substantia nigra; *SUB,* subiculum; *VL,* ventrolateral thalamic n.; *VLG,* ventrolateral geniculate n.; *VMH,* ventromedial hypothalamus; *VPL,* ventral posterolateral thalamic n.; *VPM,* ventral posteromedial thalamic n.; *ZI,* zona incerta. Note: some apparent differences between treatment groups may result from differences in the level of sectioning. See Table 4 for quantitative comparisons of hybridization signals.

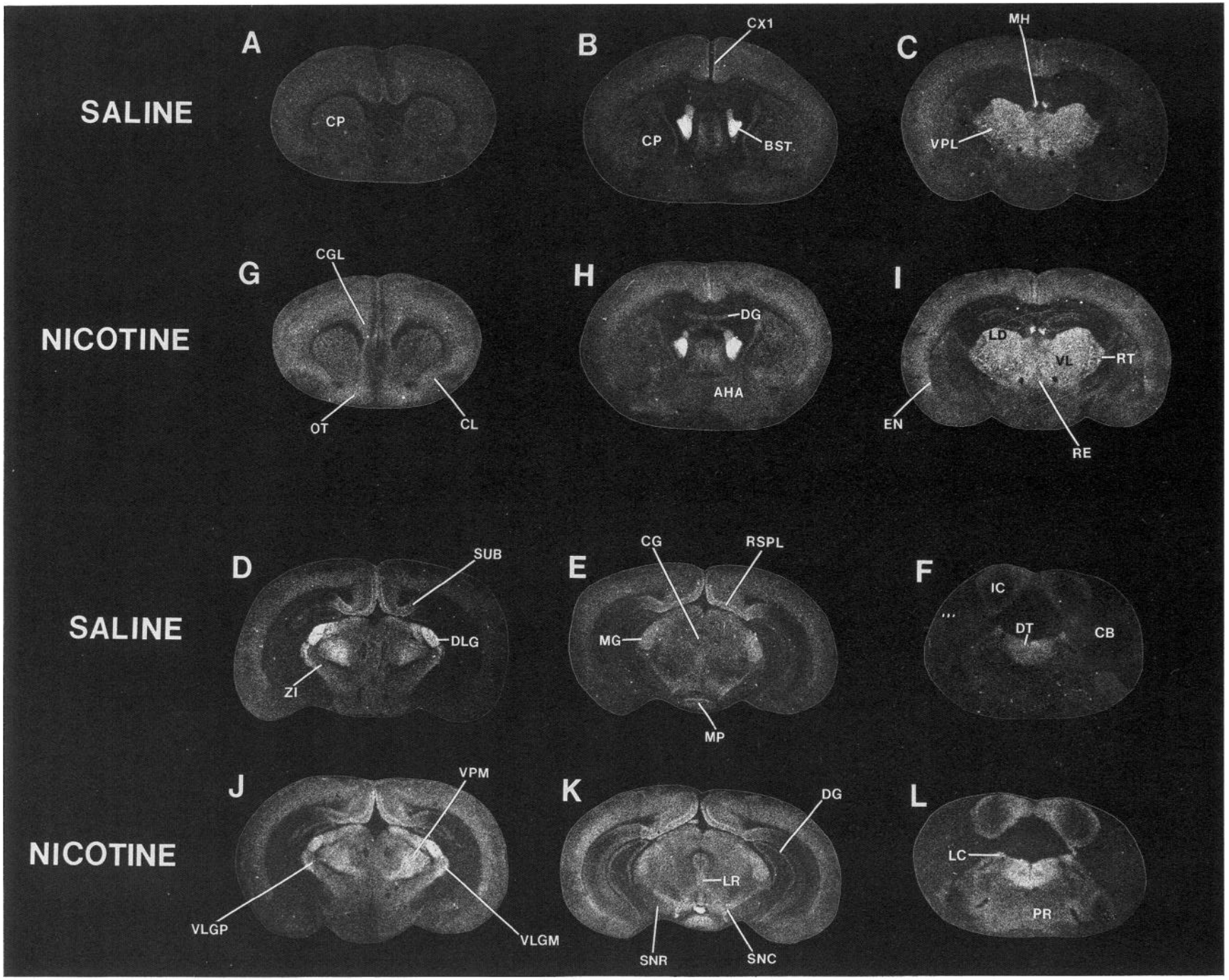
A
B
C
SALINE
CP
CP
CX1
BST
MH
VPL
G
H
I
NICOTINE
CGL
OT
CL
DG
AHA
LD
VL
RT
EN
RE
D
E
F
SALINE
SUB
DLG
ZI
CG
RSPL
MG
MP
IC
DT
CB
J
K
L
NICOTINE
VPM
VLGP
VLGM
DG
LR
SNR
SNC
LC
PR

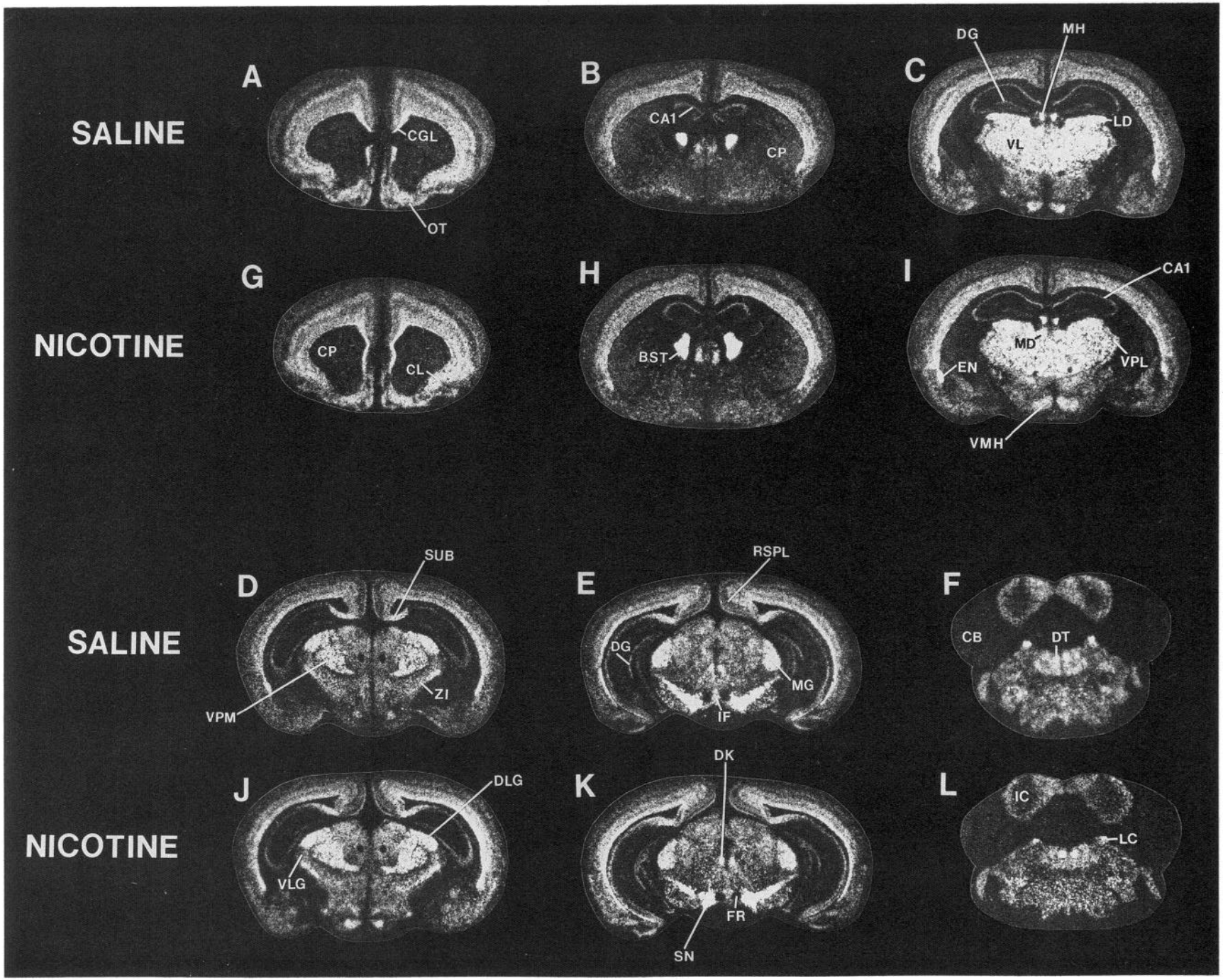
SALINE
A
CGL
OT
B
CA1
CP
C
DG
MH
LD
VL
NICOTINE
G
CP
CL
H
BST
I
CA1
MD
EN
VPL
VMH
SALINE
D
SUB
VPM
ZI
E
RSPL
DG
MG
IF
F
CB
DT
NICOTINE
J
DLG
VLG
K
DK
FR
SN
L
IC
LC

Table 3. Quantitative autoradiographic measurement of the binding of L-^{3}H-nicotine in control and nicotine-treated mice

	Control	Treated	*t*
Telencephalon			
1. Neocortex			
Cingulate cx (anterior)	38.48 ± 1.5	49.98 ± 3.4	3.09*
Cingulate cx (posterior)	39.95 ± 2.8	56.87 ± 1.4	5.40***
Entorhinal cx (dorsal)	23.99 ± 3.0	46.85 ± 5.4	3.70**
Entorhinal cx (ventral)	33.15 ± 3.5	66.96 ± 4.8	5.69***
Frontal cx (area 2)	27.63 ± 1.2	41.09 ± 4.1	3.15**
Parietal cx (layer 1)	45.21 ± 1.4	63.38 ± 2.1	7.20***
Parietal cx (layers 2–3)	22.91 ± 1.1	34.19 ± 1.5	8.73***
Parietal cx (layers 4–6)	31.61 ± 0.9	54.61 ± 1.4	13.82***
Retrosplenial cx	64.60 ± 2.4	90.72 ± 2.3	7.86***
2. Rhinencephalon			
Anterior olfactory n.	20.40 ± 1.3	43.13 ± 3.9	5.53***
Dentate gyrus	17.05 ± 1.3	36.16 ± 1.8	8.61***
Presubiculum (external)	39.84 ± 8.0	68.84 ± 6.3	2.85*
Presubiculum (internal)	58.12 ± 11.1	92.91 ± 5.2	2.84*
Subiculum (anterior)	49.25 ± 2.4	71.90 ± 2.3	5.86***
Subiculum (posterior)	67.92 ± 2.9	97.78 ± 2.3	8.24***
3. Basal ganglia			
Caudate putamen	29.71 ± 0.9	39.59 ± 1.8	4.91***
Claustrum	35.35 ± 1.3	59.73 ± 2.5	8.65***
Endopiriform n.	37.71 ± 1.3	61.70 ± 2.7	8.01***
Nucleus acumbens	24.70 ± 1.4	41.11 ± 2.4	5.91***
Olfactory tubercle	26.62 ± 1.9	45.07 ± 1.9	6.86***
Stria medullaris	75.67 ± 4.8	69.42 ± 3.7	1.03
Substantia nigra	49.10 ± 2.8	76.15 ± 2.6	7.08***
4. Septum			
Bed n. (stria terminalis)	112.94 ± 4.5	111.50 ± 4.8	0.22
Fimbrial septal n.	32.32 ± 2.4	44.14 ± 3.7	2.68*
Medial septal n.	26.45 ± 3.0	33.35 ± 1.7	2.00
Diencephalon			
1. Thalamus			
Anterior dorsal n.	85.65 ± 3.8	98.94 ± 5.6	1.96
Anterior medial n.	102.59 ± 3.1	104.95 ± 7.0	0.31
Anterior ventral n.	119.39 ± 2.5	121.81 ± 2.0	0.76
Centromedial n.	61.77 ± 3.3	70.46 ± 4.3	1.60
Laterodorsal n.	85.23 ± 3.0	97.01 ± 6.5	1.65
Mediodorsal n.	76.10 ± 2.5	86.66 ± 6.5	1.63
Parafascicular n.	46.55 ± 3.4	63.23 ± 2.2	3.22**
Paratenial n.	69.81 ± 3.9	79.87 ± 5.6	1.47
Paraventricular n.	44.03 ± 2.3	63.08 ± 3.4	4.64***
Posterior laterodorsal n.	68.24 ± 5.0	85.93 ± 3.1	3.01*
Reticular n.	59.27 ± 3.0	64.92 ± 1.0	1.79
Reunions n.	60.72 ± 2.7	77.05 ± 4.9	2.92*
Rhomboid n.	93.35 ± 3.9	103.46 ± 3.8	1.86
Ventral posterolateral n.	54.55 ± 1.6	66.94 ± 1.4	5.83***
Ventral reunions n.	78.27 ± 3.9	91.16 ± 3.2	2.56*
Ventrolateral n.	76.03 ± 2.7	81.73 ± 5.0	1.00
Ventromedial n.	67.75 ± 3.9	68.73 ± 2.6	0.21
Ventroposterior medial n.	74.59 ± 3.1	87.93 ± 1.7	3.77**
2. Epithalamus and subthalamus			
Medial habenula	101.26 ± 2.9	105.39 ± 5.4	0.69
Zona incerta (dorsal)	32.41 ± 3.1	48.06 ± 1.2	4.71***
Zona incerta (ventral)	40.98 ± 3.1	58.25 ± 1.9	4.75***
3. Metathalamus			
Anterior pretectal n.	36.25 ± 3.6	63.67 ± 3.6	5.39***
Dorsal LGN	109.54 ± 3.3	112.72 ± 3.4	0.67

Table 3. Continued

	Control	Treated	t
Lateral pretectal n.	75.37 ± 3.9	89.47 ± 3.5	2.69*
Medial geniculate	61.62 ± 2.4	85.98 ± 3.3	5.96***
Optic tract n.	110.91 ± 2.6	105.78 ± 3.4	1.20
Precommissural n.	47.53 ± 1.5	80.56 ± 2.5	11.33***
Vlg (magnocellular)	85.91 ± 4.7	98.14 ± 3.4	2.11
Vlg (parvocellular)	48.89 ± 3.6	69.91 ± 1.2	5.30***
4. Hypothalamus			
Anterior hypothalamic area	21.64 ± 1.5	36.49 ± 1.9	6.13***
Basal region	18.74 ± 1.5	35.91 ± 3.7	4.30**
Medial mammillary n.	28.01 ± 3.8	45.06 ± 3.5	3.31**
Posterior n.	37.80 ± 2.7	65.88 ± 4.4	5.43***
Supramammillary n.	49.08 ± 4.4	74.47 ± 3.3	4.62***
Mesencephalon			
Caudal linear raphe	39.07 ± 3.6	62.78 ± 6.2	3.31**
Central gray (dorsal)	41.70 ± 2.1	69.21 ± 3.2	7.19***
Central gray (ventral)	35.46 ± 2.9	59.07 ± 3.4	5.28***
Dorsal raphe	59.41 ± 5.4	83.50 ± 5.3	3.06*
Ic (external)	29.54 ± 2.9	59.74 ± 5.4	4.93***
Ic (internal)	9.73 ± 1.8	24.12 ± 3.3	3.83**
Ic (posterior)	27.29 ± 3.0	50.52 ± 2.8	5.66***
Ipn (apical)	174.38 ± 6.6	182.25 ± 7.7	0.80
Ipn (caudal)	154.59 ± 2.4	153.91 ± 13.0	0.04
Ipn (central)	159.00 ± 6.6	168.22 ± 8.2	0.88
Ipn (dorsomedial)	167.76 ± 5.2	177.04 ± 8.7	0.92
Ipn (lateral)	131.45 ± 3.7	140.62 ± 4.6	1.55
Ipn (rostral)	146.05 ± 1.5	154.67 ± 4.7	1.52
Medial raphe (anterior)	50.26 ± 2.0	68.24 ± 3.4	4.04**
Medial raphe (posterior)	43.83 ± 4.1	64.32 ± 4.2	3.49**
Microcellular tegmental n.	41.85 ± 4.9	69.71 ± 4.0	4.04**
Paranigral area	56.28 ± 3.5	80.98 ± 5.7	3.69**
Prerubral field	23.24 ± 2.7	48.79 ± 2.8	6.57***
Rhabdoid nucleus	83.67 ± 0.8	103.92 ± 7.0	2.61*
Rostral linear raphe	41.88 ± 2.0	71.44 ± 2.5	9.23***
Sc (optic nerve)	50.26 ± 1.5	78.03 ± 2.9	8.51***
Sc (superficial gray)	77.26 ± 2.0	105.67 ± 2.5	8.77***
Ventral tegmental area	35.98 ± 1.6	51.66 ± 2.6	5.14***
Pons			
Dorsal tegmental n.	57.53 ± 4.3	76.84 ± 4.0	3.29**
Laterodorsal tegmental n.	47.31 ± 4.9	60.28 ± 7.3	2.48*
Locus coeruleus	31.72 ± 2.3	52.60 ± 6.1	3.20**
Pyramidal tract	34.09 ± 2.5	59.21 ± 2.9	6.56***
Superior olivary n.	21.20 ± 2.5	28.59 ± 4.0	1.56
Medulla			
Cuneiform n.	40.99 ± 9.3	62.57 ± 5.9	2.05
Hypoglossal n.	45.68 ± 4.1	64.24 ± 3.9	3.31*
Medial vestibular n.	23.26 ± 3.3	32.11 ± 2.8	2.26*
Reticular n.	16.24 ± 1.8	25.86 ± 4.2	2.27*
Cerebellum			
Cerebellar lobules	1.99 ± 0.6	4.55 ± 1.4	1.68

Data show ^{3}H-nicotine binding in various brain regions from animals that were infused chronically with saline (control; $n = 6$) or nicotine (treated; 4.0 mg/kg/hr nicotine; $n = 6$) for 10 d. Quantitative autoradiography was performed as described in Materials and Methods. The groups were compared by t test. Asterisks designate statistically significant differences from control binding (*, 0.05 level; **, 0.01; ***, 0.001). The following abbreviations are used: cx, cortex; vlg, ventral lateral geniculate; ic, inferior colliculus; n., nucleus; sc, superior colliculus; ipn, interpeduncular nucleus.

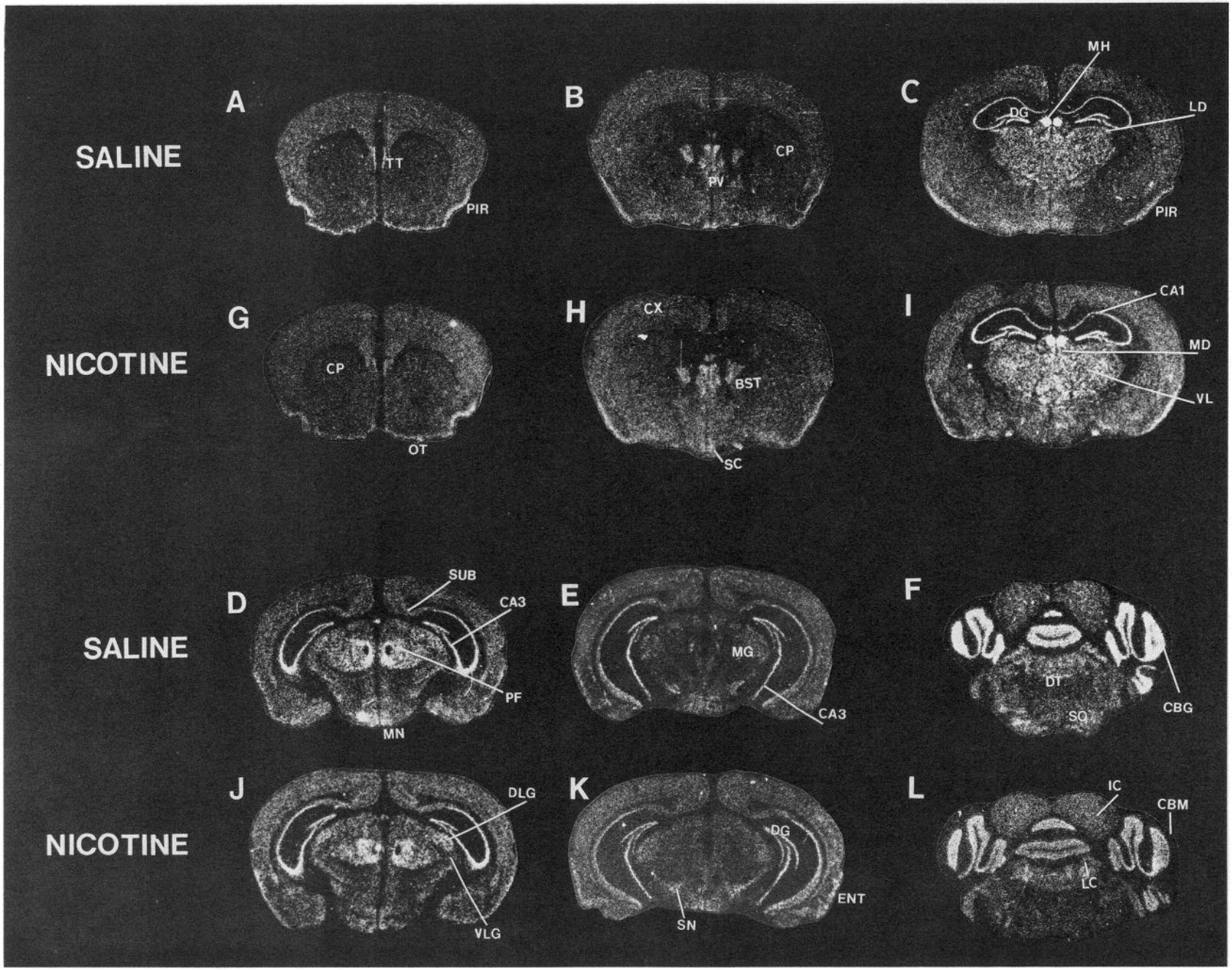
SALINE
A
TT
PIR
B
CP
PV
C
MH
DG
LD
PIR
NICOTINE
G
CP
OT
H
CX
BST
SC
I
CA1
MD
VL
SALINE
D
SUB
CA3
PF
MN
E
MG
CA3
F
DT
SO
CBG
NICOTINE
J
DLG
VLG
K
DG
ENT
SN
L
IC
CBM
LC

neocortical regions of the telencephalon. No obvious differences in the intensity of hybridization were observed in layers of the frontal or the occipital cortex, but the inner layer of the parietal cortex showed more intense hybridization than did the outer layer. Many areas in the rhinencephalon had a positive hybridization signal, with the dentate gyrus, the CA2 layer of hippocampus, and the lateral olfactory tubercle being the regions mostly intensely labeled. The substantia nigra pars compacta and pars lateralis were the most highly labeled areas in the basal ganglion, and the caudate putamen was the region showing the lowest signal. The medial septum was much more intensely labeled than was the lateral septum.

As was the case with hybridization with α_4, diencephalic regions were among the most intensely labeled with the β_2-probe. Many thalamic, metathalamic, and hypothalamic nuclei, as well as the medial and dorsal lateral geniculate, showed strong hybridization signals. The strong hypothalamic signals obtained for β_2 contrast with the relatively weak signals observed for α_4 in this brain area. The medial habelula was the most intensely labeled nucleus in the brain.

Several mesencephalic and pontine nuclei displayed moderate to strong hybridization signals, with the signals observed in the interpeduncular nucleus, the subbrachial nucleus, the dorsal tegmental nucleus, the locus coeruleus, and the superior olivary nucleus being particularly strong. In marked contrast to the absence of hybridization of α_4-probe observed in cerebellum, the hybridization intensity for the β_2-probe in the granule cell layer of the cerebellum was very strong.

The values measured for β_2-hybridization in mice infused with saline or 4.0 mg/kg/hr nicotine are summarized in Table 5. In addition, the effect of nicotine infusion on the hybridization patterns is illustrated in Figure 3 (panels *A–F* for control mice and panels *G–L* for treated mice). The intensity of hybridization observed for β_2 was unaffected in 82 of 84 brain areas analyzed, but in the dorsomedial nucleus of the hypothalamus and the lateral portion of the interpeduncular nucleus, mice that had been chronically treated with nicotine had significantly lower signals than saline-treated mice.

The average variation (SE) in signal intensity within a given area was 9.3% of the mean for control mice and 9.4% of the mean for nicotine-treated mice. On average, the signal measured for α_4-hybridization for nicotine-treated mice was 1.7% lower than that measured for control mice.

Summary of treatment effects on nicotine binding and α_4- and β_2-hybridizations. In order to provide a direct comparison of the magnitude of the effects of chronic nicotine treatment on L-^{3}H-nicotine binding and on α_4- and β_2-hybridization, frequency histograms were constructed (Fig. 4). The percentage change in signal intensity for all brain areas analyzed was calculated for each probe, and the major anatomical subdivisions for the brain regions are illustrated by different shading.

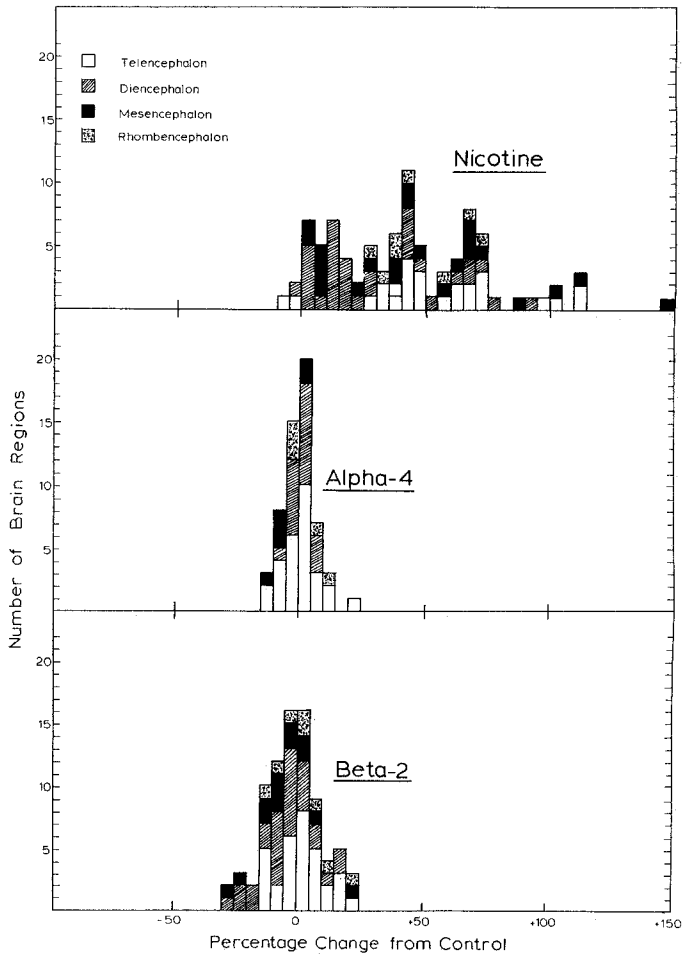

Figure 4. Relative L-^{3}H-nicotine binding and α_4 and β_2 hybridization after nicotine treatment. Relative signal intensity after chronic nicotine infusion was calculated by dividing the mean value for ligand binding or probe hybridization measured in drug-treated mice by the mean value measured for saline-treated mice for each brain area that was quantitated. Results are presented as frequency histograms of the number of brain areas displaying changes from control values indicated on the abscissa. The location within a major anatomical division of each brain region quantitated is illustrated by the differential shading of the blocks.

The results presented in Figure 4 for L-^{3}H-nicotine binding demonstrate that the change in ligand binding occurring with chronic nicotine treatment varied markedly, with changes ranging from −8% to +147%. In general, regions in the telencephalon and the rhombencephalon were more markedly affected by chronic nicotine treatment than were regions in the diencephalon. The average increase in L-^{3}H-nicotine binding in all brain areas was 42%.

The results presented in Figure 4 for α_4-hybridization illus-

←

Figure 3. Autoradiograms for *in situ* hybridization to message for β_2. Dark-field photographs of autoradiograms of β_2 cRNA hybridization are shown at six levels for saline treatment (*A–F*) and nicotine treatment (*G–L*). Brighter images indicate more intense hybridization. Abbreviations: *BST,* bed n. of stria terminalis; *CA1,* CA1 field of hippocampus; *CA3,* CA3 field of hippocampus; *CBG,* granule cell layer of cerebellum; *CBM,* molecular layer of cerebellum; *CP,* caudate putamen; *CX,* cerebral cortex; *DG,* dentate gyrus; *DLG,* dorsolateral geniculate; *DT,* dorsal tegmental n.; *ENT,* entorhinal cortex; *IC,* inferior colliculus; *LC,* locus coeruleus; *LD,* laterodorsal thalamic n.; *MD,* mediodorsal thalamic n.; *MG,* medial geniculate; *MH,* medial habenula; *MN,* mammillary n.; *OT,* olfactory tubercle; *PF,* parafascicular thalamic n.; *PIR,* piriform cortex; *PV,* paraventricular thalamic n.; *SC,* suprachiasmatic n.; *SN,* substantia nigra; *SUB,* subiculum; *SO,* superior olivary nuclei; *VL,* ventrolateral thalamic n.; *VLG,* ventrolateral geniculate; *TT,* tenia tecta. Note: some apparent differences between treatment groups may result from differences in the level of sectioning. See Table 4 for quantitative comparisons of hybridization signals.

Table 4. Relative quantitation of hybridization of cRNA transcribed from IHYA23-1E(2) (α_4) after chronic treatment with saline or nicotine

	Control	Treated	*t*
Telencephalon			
1. Neocortex			
Cingulate cortex	928.4 ± 75.1	894.7 ± 101.7	0.25
Cingulate (lateral)	2009.7 ± 136.0	1938.8 ± 161.8	0.34
Cingulate (medial)	926.6 ± 83.1	850.7 ± 60.9	0.74
Frontal cortex (area 2)	1064.2 ± 108.1	1035.9 ± 96.4	0.20
Frontal cortex (deep)	1322.7 ± 84.8	1207.4 ± 74.4	1.02
Frontal cortex (mid 1)	1102.9 ± 83.5	1120.4 ± 67.9	0.16
Frontal cortex (mid 2)	912.1 ± 82.2	855.8 ± 46.6	0.60
Frontal cortex (outer)	432.9 ± 53.5	409.2 ± 30.0	0.39
Parietal cortex (inner)	1208.1 ± 74.3	1225.0 ± 62.0	0.18
Parietal cortex (outer)	377.5 ± 33.5	397.0 ± 29.1	0.44
Occipital cortex (inner)	1546.5 ± 70.0	1557.1 ± 95.2	0.09
Occipital cortex (mid)	1072.7 ± 58.4	1044.0 ± 58.8	0.35
Orbital cortex	1292.4 ± 198.3	1292.8 ± 145.9	0.00
Retrosplenial cortex	1359.1 ± 60.0	1374.3 ± 78.7	0.15
2. Rhinencephalon			
Anterior olfactory n.	1470.7 ± 206.9	1315.1 ± 197.7	0.54
Hippocampus	111.3 ± 5.8	120.4 ± 7.9	0.92
Olfactory tubercle	672.9 ± 53.8	631.7 ± 28.9	0.71
Presubiculum	2020.9 ± 214.7	1949.1 ± 124.5	0.29
Subiculum	1782.3 ± 96.3	1790.6 ± 95.4	0.06
Subiculum (internal)	860.8 ± 57.4	784.8 ± 51.7	0.99
3. Basal ganglia			
Caudate putamen	228.5 ± 21.5	212.8 ± 17.9	0.57
Claustrum	1636.3 ± 122.7	1753.8 ± 145.9	0.60
Endopiriform	1922.1 ± 109.3	1964.0 ± 128.2	0.24
Substantia nigra (lateralis)	4030.2 ± 305.3	4512.0 ± 348.3	1.04
Substantia nigra (compacta)	4508.3 ± 411.7	4846.3 ± 301.6	0.66
4. Septum			
Fimbrial n.	1460.8 ± 50.9	1487.5 ± 186.3	0.12
Lateral septum	718.9 ± 72.6	820.1 ± 77.1	0.60
Medial septum	1668.1 ± 242.5	2037.1 ± 157.6	1.28
Triangular septal n.	3547.3 ± 244.6	3591.3 ± 292.8	0.11
Diencephalon			
1. Thalamus			
Centromedial n.	2125.6 ± 136.2	2158.3 ± 129.7	0.17
Mediodorsal n.	2696.7 ± 158.4	2720.3 ± 136.3	0.11
Posterior n.	1188.2 ± 88.6	1248.5 ± 85.9	0.49
Reunions n.	1994.3 ± 157.8	2033.0 ± 158.5	0.17
Ventral posterolateral n.	1320.1 ± 46.1	1307.2 ± 52.0	0.18
Ventral posteromedial n.	2105.9 ± 133.2	2168.4 ± 136.6	0.20
Ventrolateral n.	2098.4 ± 126.9	2118.1 ± 116.6	0.11
2. Epithalamus and subthalamus			
Medial habenula	3120.9 ± 296.1	3303.1 ± 213.0	0.50
Zona incerta	1382.7 ± 50.2	1440.9 ± 112.5	0.47
3. Metathalamus			
Anterior pretectal area	1106.4 ± 73.7	1040.9 ± 55.2	0.71
Dorsal LGN	2618.0 ± 161.5	2593.7 ± 168.8	0.10
Dorsal pretectal area	497.1 ± 12.3	485.5 ± 53.6	0.23
Lateral pretectal area	2204.3 ± 158.1	2264.8 ± 148.6	0.28
Medial geniculate n.	2268.1 ± 122.3	2215.9 ± 118.6	0.31
Olfactory tract	263.2 ± 21.9	258.9 ± 52.9	0.06
Precommissural n.	1573.6 ± 144.6	1520.9 ± 130.9	0.27
4. Hypothalamus			
Ventromedial n.	1359.0 ± 152.9	1481.6 ± 129.0	0.62
Posterior area	1346.7 ± 93.5	1405.4 ± 191.7	0.28

Table 4. Continued

	Control	Treated	t
Mesencephalon			
Caudal linear raphe	1449.6 ± 66.7	1288.6 ± 96.7	1.37
Central gray	1206.6 ± 63.2	1088.5 ± 59.6	1.36
Darkschewitsch n.	1929.9 ± 114.7	1944.7 ± 121.9	0.97
Inferior colliculus	967.9 ± 60.5	977.8 ± 73.7	0.10
Interpeduncular n.	1410.9 ± 132.2	1300.0 ± 79.1	0.77
Lateral central gray	1195.5 ± 68.3	1118.8 ± 74.6	0.76
Pons			
Dorsal tegmental n.	1830.4 ± 85.5	2048.7 ± 157.7	1.22
Laterodorsal tegmental n.	2509.5 ± 167.4	2611.9 ± 138.0	0.47
Locus coeruleus	1281.1 ± 83.8	1222.4 ± 68.3	0.54
Pontine n.	1422.7 ± 127.4	1366.3 ± 71.5	0.83
Reticular n.	626.3 ± 42.3	613.9 ± 53.5	0.18
Cerebellum			
Cerebellum	91.2 ± 7.2	82.9 ± 9.2	0.71

Data show hybridization of ^{35}S-cRNA for α_4 in various brain regions from animals that were infused chronically with saline (control; $n = 6$) or nicotine (treated; 4.0 mg/kg/hr nicotine; $n = 6$) for 10 d. Quantitative autoradiography was performed as described in Materials and Methods. The groups were compared by t test. No statistically significant effects of treatment were observed. Signal intensity measured in hippocampus and cerebellum do not differ from film background and represent nonspecific hybridization.

trate that chronic treatment resulted in little change in signal intensity for this probe, since the percentage changes cluster around zero. The average change observed for all regions was a 0.1% decrease, while the extreme changes observed were a 13% decrease and a 22% increase in signal intensity. No significant changes in signal intensity were found. No overall trend toward either an increase or decrease in α_4 was evident.

The results presented in Figure 4 for the effect of nicotine treatment on β_2-hybridization are similar to those found for α_4: the percentage changes cluster around zero with an overall average decrease of 1.3% occurring after chronic nicotine treatment. The distribution observed for β_2 is broader than that observed for α_4, reflecting, in part, the slightly larger error encountered in quantitating β_2-signal. Extreme changes were a 30% decrease and a 22% increase in signal intensity. Two changes were statistically significant, the 30% decrease found in the lateral portion of the interpeduncular nucleus and the 20% decrease found in the dorsomedial hypothalamus. No overall trend toward either an increase or a decrease in β_2-hybridization was indicated.

In situ *hybridizations, other α-subunits.* Although α_4 represents most of the nicotinic receptors measured with high-affinity L-^{3}H-nicotine binding, other α-subunits exist in brain that may encode a small percentage of L-^{3}H-nicotine binding sites and may respond to chronic nicotine treatment in a manner different from that observed for α_4. In order to determine the effects of nicotine treatment on mRNA levels for other α-subunits, *in situ* hybridizations for α_2, α_3, and α_5 were performed. Coronal sections illustrating the distribution for hybridization of α_2, α_3, and α_5-cRNA probes at several brain levels for saline-infused mice are presented in Figure 5.

α_2. The pattern of α_2-hybridization is illustrated in Figure 5*A–C*. The full-length cRNA probe used for hybridization tended to give relatively high background, in contrast to the probes used for the other α-subunits. Very high-stringency wash (0.1 × SSC, 80°C, 30 min) substantially reduced the background without obvious effect on the three nuclei that showed the strongest hybridization: interpeduncular nucleus and ventral and dorsal tegmental nuclei. These nuclei, in fact, were the only mouse brain areas with signals significantly exceeding background. The quantitative determination of the signals is summarized in Table 6.

The interpeduncular nucleus and tegmental nuclei demonstrated signals substantially higher than background for both saline- and nicotine-treated mice. Chronic treatment had no significant effect on the extent of hybridization in any region.

The average variation (SE) in signal intensity for control and treated mice in the two regions displaying detectable hybridization was 11.6%. On average, the signal measured for α_2-hybridization for nicotine-treated mice was 8% lower than that measured for control mice.

α_3. The pattern for α_3-hybridization is presented in Figure 5*D–F*. Hybridization that exceeded background was detected in several areas of telencephalon, diencephalon, mesencephalon, and pons. An extremely high concentration of α_3-mRNA was detected in the medial habenula; the signal in the habenula was 20-fold greater than that in the motor trigeminal nucleus, the region expressing the second highest level of mRNA (see Table 7).

Chronic nicotine treatment had no significant effect on α_3-hybridization in any brain region as shown in Table 7.

The average variation (SE) in signal intensity within a given area was 9.0% of the mean for control mice and 10.9% of the mean for nicotine-treated mice. On average, the signal measured for α_3-hybridization for nicotine-treated mice was 2% lower than that measured for control mice.

α_5. The pattern for α_5-hybridization is illustrated in Figure 5*G–I*. α_5-mRNA was detectable in the telencephalon (cortical layer six), the rhinencephalon (subiculum and dentate gyrus), the diencephalon (medial habenula), the mesencephalon (substantia nigra and interpeduncular nucleus), and in the pons (pyramidal tract and dorsal tegmental nucleus).

Chronic nicotine treatment had no significant effect on the signal intensity for α_5 in any brain area analyzed (see Table 8).

The average variation (SE) in signal intensity within a given area was 9.9% of the mean for control mice and 11.4% of the

Table 5. Relative quantitation of hybridization of cRNA transcribed from pSP65-49 (β_2) after chronic treatment with saline or nicotine

	Control	Treated	*t*
Telencephalon			
1. Neocortex			
Entorhinal cortex	205.2 ± 14.9	195.3 ± 13.3	0.50
Frontal cortex (inner)	176.3 ± 17.8	214.5 ± 29.8	1.09
Frontal cortex (outer)	153.8 ± 8.8	182.7 ± 22.6	1.08
Cingulate cortex	225.6 ± 19.1	252.4 ± 27.1	0.81
Occipital cortex	200.5 ± 24.2	216.2 ± 13.2	0.60
Parietal cortex (inner)	227.6 ± 17.0	248.8 ± 18.7	0.82
Parietal cortex (outer)	173.8 ± 13.2	194.9 ± 16.5	1.00
Retrosplenial cortex	253.1 ± 22.4	263.5 ± 16.0	0.38
Pyriform cortex	345.0 ± 16.3	307.6 ± 20.4	1.43
2. Rhinencephalon			
Anterior olfactory n.	231.2 ± 30.8	247.4 ± 34.9	0.34
Dentate gyrus	434.8 ± 37.9	429.0 ± 32.3	0.12
Hilus of dentate gyrus	64.7 ± 4.2	68.7 ± 6.4	0.53
Hippocampus (CA1)	308.9 ± 23.7	312.8 ± 22.6	0.12
Hippocampus (CA2)	530.5 ± 47.1	550.3 ± 48.6	0.29
Hippocampus (CA3)	403.1 ± 31.8	391.8 ± 26.5	0.27
Olfactory tubercle (medial)	288.9 ± 23.4	309.5 ± 22.5	0.63
Olfactory tubercle (lateral)	414.2 ± 21.8	381.0 ± 21.8	1.08
Subiculum	253.1 ± 22.4	263.5 ± 16.0	0.38
3. Basal ganglia			
Anterior cortical amygdala	312.4 ± 25.7	368.0 ± 46.0	0.91
Caudate putamen	112.1 ± 5.1	131.1 ± 12.1	1.45
Diagonal band	308.7 ± 23.7	293.6 ± 23.1	0.46
Medial amygdala	350.9 ± 26.7	313.2 ± 20.1	1.10
Substantia nigra (compacta)	461.8 ± 46.7	411.2 ± 24.6	0.96
Substantia nigra (lateralis)	394.8 ± 41.5	379.1 ± 25.0	0.38
4. Septum			
Bed n. (stria terminalis)	234.7 ± 19.6	244.5 ± 25.6	0.30
Lateral	196.0 ± 17.4	191.4 ± 22.0	0.05
Medial	502.7 ± 57.8	590.0 ± 77.8	0.91
Diencepahlon			
1. Thalamus			
Centromedial n.	475.4 ± 48.0	486.3 ± 60.4	0.12
Laterodorsal n.	355.1 ± 21.5	393.0 ± 37.4	0.88
Lateroposterior n.	336.7 ± 31.8	295.0 ± 25.9	1.02
Mediodorsal n. (lateral)	379.8 ± 25.2	352.8 ± 27.4	0.73
Mediodorsal n. (central)	572.1 ± 56.6	556.4 ± 62.8	0.18
Optic tract n.	254.6 ± 25.8	255.7 ± 33.7	0.03
Parafascicular n.	555.1 ± 65.6	538.4 ± 34.5	0.23
Posterior n.	175.3 ± 15.3	206.7 ± 19.4	1.22
Reunions n.	502.4 ± 50.6	590.8 ± 69.2	1.03
Subthalamic n.	356.2 ± 27.7	343.5 ± 6.6	0.76
Ventromedial n.	334.0 ± 21.7	339.8 ± 27.3	0.16
Ventroposterior n.	372.2 ± 27.2	366.2 ± 28.3	0.15
Ventroposterolateral n.	234.6 ± 24.0	250.2 ± 23.9	0.46
2. Epithalamus and subthalamus			
Medial habenula (caudal)	1037.8 ± 92.9	1117.3 ± 109.3	0.29
Medial habenula (rostral)	634.0 ± 78.8	583.3 ± 59.5	0.52
Zona incerta	278.6 ± 18.5	264.7 ± 19.0	0.53
3. Metathalamus			
Dorsolateral geniculate	426.0 ± 32.7	383.7 ± 29.6	0.96
Medial geniculate	364.7 ± 27.0	359.3 ± 23.5	0.15
Ventrolateral geniculate	225.0 ± 20.9	202.2 ± 17.3	0.84

Table 5. Continued

	Control	Treated	t
4. Hypothalamus			
Dorsomedial n.	407.2 ± 25.6	325.5 ± 25.9	2.24*
Mammillary n.	405.4 ± 48.9	331.8 ± 20.0	1.39
Periventricular area	351.4 ± 26.3	338.7 ± 25.6	0.34
Posterior n.	255.8 ± 23.1	221.7 ± 22.7	1.05
Premammillary n. (dorsal)	518.3 ± 69.2	375.3 ± 37.1	1.91
Premammillary n. (ventral)	539.5 ± 54.4	415.8 ± 40.6	1.82
Suprachiasmatic n.	487.1 ± 35.8	462.5 ± 57.9	0.39
Supramammillary n.	335.5 ± 74.3	305.4 ± 26.9	0.42
Ventromedial n.	373.4 ± 10.9	380.4 ± 31.6	0.21
Mesencephalon			
Anterior pretectal area	309.2 ± 34.3	282.6 ± 49.4	0.46
Central gray (dorsal)	230.1 ± 16.9	231.0 ± 18.1	0.03
Central gray (ventral)	313.7 ± 24.1	308.1 ± 28.5	0.15
Darkschewitsch n.	309.8 ± 38.3	281.2 ± 27.4	0.61
Inferior colliculus	264.3 ± 20.4	282.0 ± 25.5	0.54
Interpeduncular n. (medial)	505.5 ± 56.9	443.8 ± 63.5	0.72
Interpeduncular n. (lateral)	440.2 ± 42.4	307.6 ± 29.7	2.56*
Linear raphe	335.9 ± 20.7	284.4 ± 18.7	1.85
Subbrachial n.	416.5 ± 16.6	326.6 ± 45.7	1.61
Superior colliculus	293.7 ± 14.7	290.3 ± 25.7	0.12
Ventral tegmental area	255.1 ± 30.0	260.4 ± 42.1	0.10
Pons			
Dorsal tegmental n.	457.1 ± 53.1	435.5 ± 39.8	0.33
Laterodorsal tegmental n.	293.5 ± 17.0	327.6 ± 26.5	1.03
Locus coeruleus	531.6 ± 69.6	538.2 ± 51.7	0.08
Preolivary n. (caudal)	254.8 ± 41.9	232.0 ± 21.2	0.54
Preolivary n. (rostral)	297.2 ± 23.5	358.9 ± 29.6	1.01
Pontine n.	344.1 ± 39.6	305.9 ± 40.3	0.68
Superior olivary n.	486.6 ± 110.0	532.2 ± 88.1	0.32
Trigeminal n.	242.3 ± 19.7	245.9 ± 19.7	0.13
Cerebellum			
Granule cell layer	673.1 ± 50.9	626.7 ± 71.2	0.53
Molecular layer	86.2 ± 5.8	86.7 ± 5.4	0.06
Miscellaneous			
Anterior commissure	73.7 ± 10.9	86.8 ± 14.7	0.68
Corpus callosum (forceps mn)	88.1 ± 14.2	88.3 ± 10.1	0.01
Infralimbic cortex	325.0 ± 21.1	324.5 ± 32.2	0.01
Choroid plexus	681.1 ± 73.3	583.2 ± 67.3	0.98
Corticospinal tract	305.9 ± 33.6	271.0 ± 33.1	0.74

Data show hybridization of ^{35}S-cRNA for β_2 in various brain regions from animals that were infused chronically with saline (control; $n = 6$) or nicotine (treated; 4.0 mg/kg/hr nicotine; $n = 6$) for 10 d. Quantitative autoradiography was performed as described in Materials and Methods. The groups were compared by t test. Statistically significant effects of treatment were observed in two brain areas marked with asterisks. Signal intensity measured in the hilus of the dentate gyrus, anterior commissure, corpus callosum, and light areas of cerebellum does not differ from film background and represents nonspecific hybridization.

mean for nicotine-treated mice. On average, the signal measured for α_5-hybridization for nicotine-treated mice was 12.5% higher than that measured for control mice.

Discussion

It has been previously demonstrated that chronic exposure to nicotine results in an increase in the numbers of putative nicotinic receptors measured by the binding of radiolabeled nicotinic agonists such as nicotine or ACh in mouse (Marks et al., 1983, 1985, 1986a), rat (Schwartz and Kellar, 1983), and human (Benwell et al., 1988) brain. The results of the present study confirm these observations. The results also indicate that the increase in L-^{3}H-nicotine binding is not universal: many regions in the diencephalon, as well as the interpeduncular nucleus, were unaffected by chronic treatment. The differential response of nicotinic sites to chronic nicotine treatment in different brain areas is consistent with the observations made in rat brain (Kellar et al., 1989) and mouse brain (Pauly et al., 1991). The mechanism by which the increase in receptor number occurs and the reasons for the differential response in different brain areas are, as yet, unknown. One possible explanation is that the increase in receptors is regulated by an increase in transcription or stabilization of the mRNA, resulting in an elevation of the amount of RNA encoding the receptor subunits.

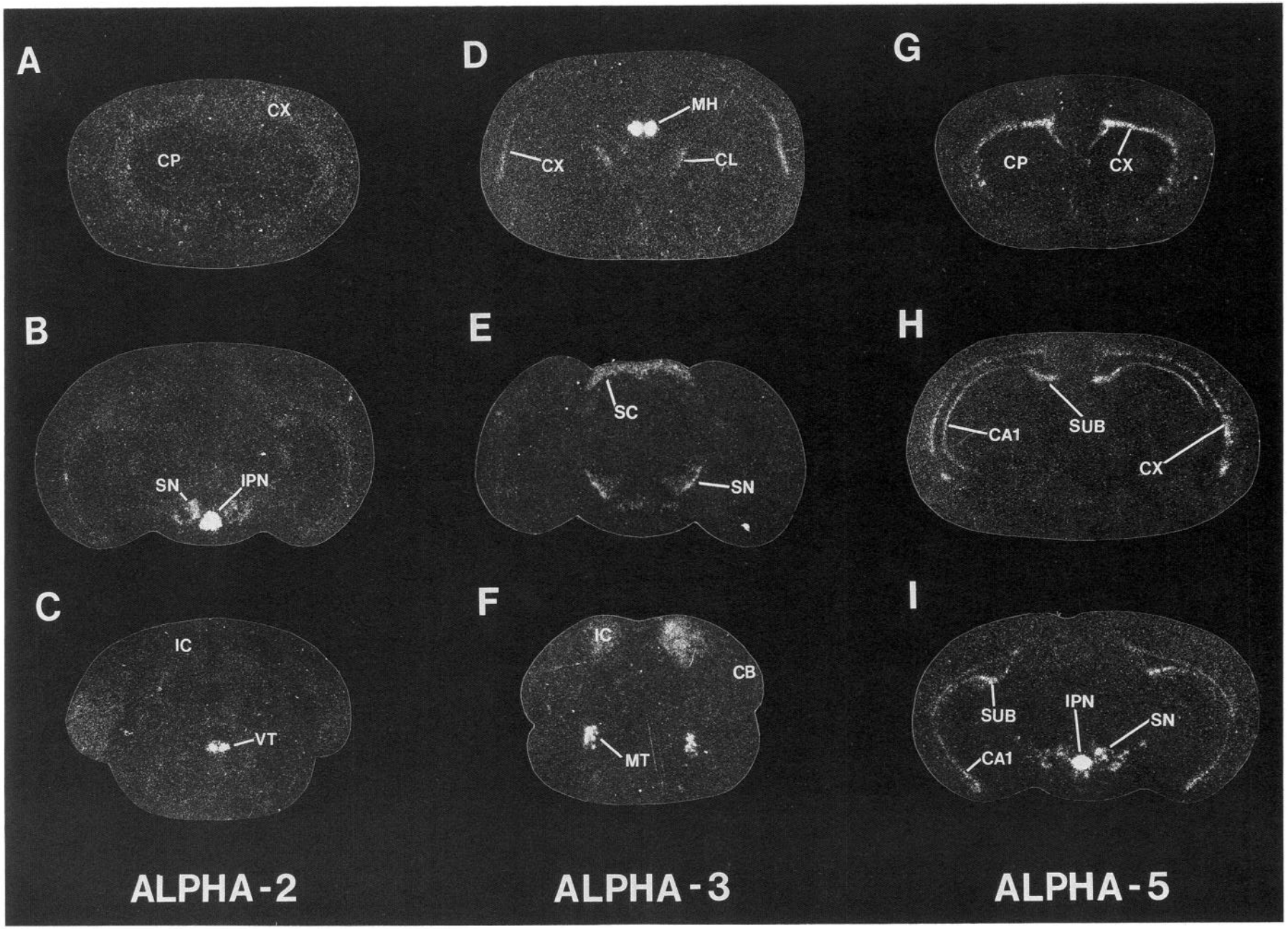
A
CX
CP
B
SN
IPN
C
IC
VT
D
MH
CX
CL
E
SC
SN
F
IC
CB
MT
G
CP
CX
H
CA1
SUB
CX
I
SUB
IPN
SN
CA1
ALPHA-2
ALPHA-3
ALPHA-5

Table 6. Relative quantitative hybridization of cRNA transcribed from pHYP16(rev) (α_2) after chronic saline or nicotine treatment

	Control	Treated	t
Telencephalon			
1. Rhinencephalon			
Hippocampus	98.9 ± 8.1	115.5 ± 9.5	1.33
2. Basal ganglia			
Caudate putamen	98.5 ± 11.0	113.1 ± 9.8	0.99
Mesencephalon			
Interpeduncular n.	1511.1 ± 284.0	1440.4 ± 141.9	0.22
Pons			
Tegmental n.			
(dorsal and ventral)	1681.4 ± 233.8	1495.2 ± 61.4	0.77

Data show hybridization of ^{35}S-cRNA for α_2 in various brain regions from animals that were infused chronically with saline (control; $n = 6$) or nicotine (treated; 4.0 mg/kg/hr nicotine; $n = 6$) for 10 d. Quantitative autoradiography was performed as described in Materials and Methods. The groups were compared by t test. No significant effects of treatment were observed. Image intensity measured in hippocampus and caudate putamen represents background hybridization and does not differ from film background.

The goal of the present study was to determine whether chronic nicotine treatment affected the level of RNA encoding several subunits of nicotinic cholinergic receptors in mouse brain. The time of treatment and the dose of nicotine used were chosen to result in maximal increases in L-^{3}H-nicotine binding sites in mouse brain; that is, the receptor levels were at steady state. While most of the receptors that bind nicotine with high affinity in adult rodent brain appear to be composed of a single subtype (α_4, β_2) (Whiting and Lindstrom, 1986; Whiting et al., 1987; Lindstrom et al., 1990), other subunits may contribute minor components of nicotine binding. Therefore, in addition to α_4 and β_2, other α-subunits known at the time this study was undertaken (α_2, α_3, and α_5) were measured as well. The results obtained in the present study strongly suggest that chronic nicotine infusion of mice does not result in a steady-state increase (or decrease) in the amount of RNA coding for α_4-subunit, which is likely to be the major agonist-binding subunit responsible for high-affinity nicotine binding, or in a change in the levels of RNA for three other, less widely distributed, α-subunits. Similarly, chronic nicotine treatment had little effect on the amount of RNA encoding the β_2-subunit, which is the likely major structural subunit in the nicotinic receptor complex measured with L-^{3}H-nicotine binding. The premise that high-affinity L-^{3}H-nicotine binding measures nicotinic receptors composed of α_4- and β_2-subunits is also supported by studies in which antibodies prepared to the cytoplasmic domain of both the α_4- and β_2-subunits precipitate the binding sites both before and after chronic nicotine treatment in rats (Flores et al., 1992).

Complete mapping of nicotinic receptor subunit protein and comparison to mRNA encoding the protein subunits have not yet been accomplished. Consequently, the correspondence between mRNA levels in a specific brain area and the protein encoded by that mRNA in the same or a different brain area remains unknown. The present study made no attempt to establish such a correspondence. In order to overcome partially the limitations imposed by absence of information on the relationship between mRNA and protein, the signal intensity for L-^{3}H-nicotine binding and nicotinic subunit mRNA was measured in as many brain areas as possible in order to determine if chronic nicotine treatment affected any or all of these measures. The results presented in Tables 3–5 and summarized in Figure 4 indicate that chronic nicotine treatment resulted in a general increase in the amount of L-^{3}H-nicotine binding, without effect on the levels of mRNA encoding either α_4- or β_2-subunits. Therefore, even though a definitive assignment of a relationship between mRNA and protein within specific brain nuclei cannot be made, the observation that mRNA levels were unaffected by chronic drug treatment strongly suggests that, if the L-^{3}H-nicotine binding measures the amount of nicotinic receptor composed of α_4- and β_2-subunits, the increase in nicotinic receptors measured by high-affinity nicotine binding is not controlled by a simple increase in transcription of mRNA or lower rate of degradation of the mRNA for the nicotinic ACh receptor subunits measured in this study.

Methods to quantitate mRNA in neural tissue by *in situ* hybridization have not been widely used. The several control experiments described in the present article suggest that *in situ* hybridization performed under controlled conditions using a single preparation of cRNA probe within an experiment and analyzed using quantitative video image analysis provides at least a relative measurement of mRNA levels. In addition, the results obtained by quantitation of the *in situ* hybridizations were consistent with the results obtained independently using solution hybridization methods.

Examination of the relative variability (as estimated by the average SE values of the measurements within each brain area) indicates that the reliability of the quantitation of mRNA levels was comparable to the reliability of the quantitation of L-^{3}H-nicotine binding. The reliability of the measurements sets the limits for detection of statistically significant changes from con-

←

Figure 5. Autoradiograms for *in situ* hybridization to message for α_2, α_3, and α_5. Dark-field photographs of autoradiograms for hybridization of cRNA for α_2 (*A–C*), α_3 (*D–F*), and α_5 (*G–I*) are shown at three different levels for each message in saline-treated mice. Brighter images indicate more intense hybridization. Abbreviations: *CA1*, CA1 region of hippocampus; *CB*, cerebellum; *CL*, centrolateral thalamic n.; *CP*, caudate putamen; *CX*, cerebral cortex; *IC*, inferior colliculus; *IPN*, interpeduncular n.; *MH*, medial habenula; *MT*, motor trigeminal n.; *SC*, superior colliculus; *SN*, substantia nigra; *SUB*, subiculum; *VT*, ventral tegmental n.

Table 7. Relative quantitative hybridization of cRNA transcribed from pPCA48E(4) (α_3) to brain regions from control and nicotine-treated mice

	Control	Treated	*t*
Telencephalon			
1. Neocortex			
Cerebral cortex (layer IV)	201.6 ± 8.5	191.1 ± 6.7	0.98
2. Rhinencephalon			
Hippocampus	71.0 ± 9.5	72.2 ± 8.2	0.10
3. Basal ganglia			
Bed n. of stria terminalis	156.2 ± 15.6	183.1 ± 47.7	0.66
Caudate putamen	75.8 ± 7.6	75.5 ± 7.2	0.99
Substantia nigra	466.6 ± 33.5	425.1 ± 45.3	0.74
Diencephalon			
1. Epithalamus and subthalamus			
Medial habenula	14,711.0 ± 1456.7	12,328.6 ± 514.6	1.54
Stria medularis	150.2 ± 7.4	175.5 ± 13.0	1.51
2. Metathalamus			
Medial geniculate n.	421.0 ± 47.8	367.1 ± 32.7	0.96
3. Hypothalamus			
Anterior hypothalamic area	198.3 ± 16.1	188.1 ± 11.3	0.49
Hypothalamus (remaining)	136.3 ± 18.6	130.0 ± 22.0	0.22
Suprachiasmatic n.	247.7 ± 29.2	269.4 ± 37.7	0.47
Ventromedial hypothalamus	396.9 ± 16.8	297.9 ± 48.5	0.30
Mesencephalon			
Inferior colliculus	475.5 ± 56.4	476.6 ± 45.8	0.01
Intercollicular area	257.0 ± 18.5	256.4 ± 19.9	0.01
Interpeduncular n.	397.9 ± 49.6	434.3 ± 60.0	0.81
Superior colliculus	516.4 ± 10.6	480.2 ± 32.8	0.56
Ventral tegmental area	80.3 ± 10.7	77.7 ± 12.0	0.16
Pons			
Medial vestibular n.	321.9 ± 58.8	302.8 ± 34.5	0.23
Motor trigeminal n.	794.7 ± 71.2	827.4 ± 100.6	1.03

Data show hybridization of ^{35}S-cRNA for α_3 in various brain regions from animals that were infused chronically with saline (control; $n = 6$) or nicotine (treated; 4.0 mg/kg/hr nicotine; $n = 6$) for 10 d. Quantitative autoradiography was performed as described in Materials and Methods. The groups were compared by *t* test. No significant effects of treatment were observed. Hybridization measured in hippocampus, caudate putamen, and ventral tegmental area represents nonspecific hybridization and does not differ from film background.

trol values after chronic nicotine treatment. The limits can be estimated from the SE values of the two groups, the value of *t* in the *t* test, and the degrees of freedom determined by the group sizes. Using these calculations, average differences between control and nicotine-treated groups of about 20% for L-^{3}H-nicotine binding, 24% for α_4-hybridization, and 31% for β_2-hybridization are required to achieve statistical significance. The average changes observed experimentally for each measure were +42%, −0.1%, and −1.7%, respectively. The comparison of relative errors of measurement and changes in signal intensity after chronic treatment strongly suggest that failure to observe changes in intensity of hybridization did not arise from fundamental differences in the reliability of measurement for the various probes.

In the absence of an effect of chronic nicotine treatment on RNA levels encoding four α-subunits or the β_2-subunit, regulation of steady-state changes in receptor levels (measured as binding sites) seems likely to result from changes in posttranscriptional processing, at least for the subunits measured. Among possible explanations for increased receptor levels in the absence of increased levels of message are increases in translational efficiency, decreases in protein degradation rates, increased incorporation of receptors from premade pools, or activation of previously inactive receptors.

Studies on the dopamine receptor system suggest that chronic drug treatment may not affect mRNA encoding various subtypes of dopamine receptors. Treatment of rats with dopamine antagonists, such as haloperidol, resulted in increases in dopaminergic receptors as measured by increases in the numbers of binding sites, but had no significant effect on mRNA encoding for these receptor proteins (van Tol et al., 1990; Xu et al., 1992). However, either chemical (Brene et al., 1990; Xu et al., 1992) or mechanical lesions (Neve et al., 1991) resulted in increases in both dopaminergic receptors and the mRNA encoding for these receptors. Similarly, axotomy of facial motoneurons changed the levels of mRNA encoding nicotinic receptors: mRNA encoding α_3 decreased while mRNA encoding β_2 increased (Senba et al., 1990). These observations, coupled with the observations made in the present study, indicate that regulation of mRNA encoding for neurotransmitter receptors differs between drug-treated and denervated tissue.

The experiments described in the present study used cRNA probes isolated from rat to measure mRNA levels in mice. Since cross-species probes were used, these probes were synthesized

Table 8. Quantitation of relative hybridization of cRNA transcribed from pPC989 (α_5) in control and nicotine-treated mice

	Control	Treated	t
Telencephalon			
1. Neocortex			
Cerebral cortex (deep)	289.2 ± 26.5	298.0 ± 17.2	0.28
2. Rhinencephalon			
Dentate gyrus	193.3 ± 14.7	209.2 ± 23.0	0.58
Hippocampus	64.4 ± 9.7	62.6 ± 6.3	0.16
Subiculum	350.7 ± 50.2	457.8 ± 76.5	1.17
3. Basal ganglia			
Caudate putamen	70.2 ± 9.8	90.3 ± 25.6	0.73
Substantia nigra	417.3 ± 32.6	484.3 ± 31.8	1.47
Diencephalon			
1. Epithalamus and subthalamus			
Medial habenula	238.3 ± 15.9	219.7 ± 8.4	1.03
Mesencephalon			
Interpeduncular n.	1421.0 ± 159.9	1638.8 ± 148.2	1.00
Ventral tegmental area	71.9 ± 12.1	67.5 ± 13.3	0.24
Pons			
Dorsal tegmental n.	874.6 ± 129.1	1196.0 ± 368.9	1.05
Pyramidal tract	257.3 ± 18.5	258.6 ± 19.2	0.05

Data show hybridization of ^{35}S-cRNA for α_5 in various brain regions from animals that were infused chronically with saline (control; $n = 6$) or nicotine (treated; 4.0 mg/kg/hr nicotine; $n = 6$) for 10 d. Quantitative autoradiography was performed as described in Materials and Methods. The groups were compared by t test. No significant effects of treatment were observed. Hybridization measured in hippocampus, caudate putamen, and ventral tegmental area represents background hybridization, and the signals do not differ from film background.

to hybridize with the full coding region of each of the mRNA subunits measured. This strategy was employed to maximize the ability to detect mRNA that may differ between rat and mouse. Since full-length probes were used, the possibility of cross-hybridization between a specific probe and other, similar, mRNA species was possible. To minimize this possibility, hybridizations and washes were conducted under very high-stringency conditions. In addition, control experiments indicated that the signals obtained after additional washes at higher stringency were comparable to the signals obtained after the initial washes for every probe except that for α_2, as indicated in the Results.

The relative intensity of the hybridization observed using the rat β_2-probe in mouse brain was much lower than that observed with the rat α_4-probe in mouse brain. In addition, less variation in signal intensity among brain areas was observed with the β_2-probe than with the α_4-probe. To determine if a misleading hybridization pattern was obtained by using a cross-species probe, two different β_2-clones were isolated from a mouse brain library and the patterns of hybridization obtained with these probes were compared to that obtained with the rat probe. The pattern of hybridization was the same for all three probes, but the intensity of the signals obtained with the mouse probes was greater than that obtained using the rat probe. Nevertheless, the results indicated that the rat probe used in the present study was adequate for the analysis of relative levels of mRNA for mouse β_2.

The results presented in the present article indicate that the distribution of mRNA encoding four α-subunits of nicotinic cholinergic receptors in mouse brain are, in general, similar to those previously reported for rat brain (Wada et al., 1989; Boulter et al., 1990), but that some qualitative and quantitative differences in the distribution of mRNA for several of these nicotinic subunits may exist. Since the experimental conditions employed for the hybridization experiments with the two species were different, detailed comparisons at the present time may be misleading. A direct comparison of the hybridization patterns for the neuronal nicotinic receptor subunit mRNAs in rat and mouse brain would be valuable.

In summary, the results presented in this article strongly suggest that the steady-state increase in nicotinic receptors that bind L-^{3}H-nicotine with high affinity that occurs with chronic nicotine treatment does not result from an increase in the amount of mRNA encoding any one of four α-subunits or from a change in a widely expressed β-subunit (β_2) of the nicotinic cholinergic receptors, although regulation of receptor level by changes in the levels of RNA encoding other nicotinic subunits has not yet been investigated. If L-^{3}H-nicotine binding measures nicotinic receptors composed of α_4- and β_2-subunits, it seems likely that regulation of receptor increases that occur with chronic nicotine treatment occurs posttranscriptionally.

References

Barr JE, Holmes DB, Ryan LM, Sharpless SH (1979) Techniques for the chronic cannulation of the jugular vein in mice. Pharmacol Biochem Behav 11:115–118.

Benwell MEM, Balfour DJK, Anderson JM (1988) Evidence that tobacco smoking increases the density of (−)-[^{3}H]nicotine binding sites in human brain. J Neurochem 50:1243–1247.

Boulter J, Evans K, Goldman D, Martin G, Treco D, Heinemann S, Patrick J (1986) Isolation of a cDNA clone coding for a possible neural nicotinic receptor α-subunit. Nature 319:368–374.

Boulter J, Connelly J, Deneris E, Goldman D, Heinemann S, Patrick J (1987) Functional expression of two neuronal nicotinic acetylcholine receptors from cDNA clones identifies a gene family. Proc Natl Acad Sci USA 84:7763–7767.

Boulter J, O'Shea-Greenfield A, Duvoisin RM, Connolly JG, Wada E, Jensen A, Gardner PD, Ballivet M, Deneris ES, McKinnon D, Heinemann S, Patrick J (1990) $\alpha 3$, $\alpha 5$ and $\beta 4$: three members of the rat neuronal nicotinic acetylcholine receptor-related gene family form a gene cluster. J Biol Chem 265:4472–4482.

Brene S, Lindefors N, Herrera-Marschitz M, Persson H (1990) Expression of dopamine D2 receptor and choline acetyltransferase mRNA in the dopamine deafferented rat caudate-putamen. Exp Brain Res 83:96–104.

Chomczynski P, Sacchi N (1987) Single-step method of RNA isolation by acid guanidinium thiocyanate-phenol-chloroform extraction. Anal Biochem 162:156–159.

Clarke PBS, Schwartz RD, Paul SM, Pert CB, Pert A (1985) Nicotinic binding in rat brain: autoradiographic comparison of [^{3}H]acetylcholine, [^{3}H]nicotine and [^{125}I]bungarotoxin. J Neurosci 5:1307–1315.

Couturier S, Bertrand D, Matter J-M, Hernandez M-C, Bertrand S, Millar N, Valera S, Barkas T, Ballivet M (1990) A neuronal nicotinic acetylcholine receptor subunit ($\alpha 7$) is developmentally regulated and forms a homo-oligomeric channel blocked by a-BTX. Neuron 5:847–856.

Cox KH, DeLeon LM, Angerer LM, Angerer RC (1984) Detection of mRNAs in sea urchin embryos by *in situ* hybridization using asymmetric RNA probes. Dev Biol 101:485–502.

Deneris ES, Connolly J, Boulter J, Wada E, Wada K, Swanson LW, Patrick J, Heinemann S (1988) Primary structure and expression of $\beta 2$: a novel subunit of neuronal nicotinic receptors. Neuron 1:45–54.

Deneris ES, Boulter J, Patrick J, Swanson LW, Heinemann S (1989) $\beta 3$: a new member of nicotinic acetylcholine receptor gene family is expressed in brain. J Biol Chem 264:6268–6272.

Duvoisin RM, Deneris ES, Boulter J, Patrick J, Heinemann S (1989) The functional diversity of the neuronal nicotinic acetylcholine receptors is increased by a novel subunit: $\beta 4$. Neuron 3:487–496.

Flores CM, Rogers SW, Pabreza LA, Wolfe BB, Kellar KJ (1992) A subtype of nicotinic cholinergic receptor in rat brain is composed of $\alpha 4$ and $\beta 2$ subunits and is up-regulated by chronic nicotine treatment. Mol Pharmacol 41:31–37.

Goldman D, Deneris E, Luyten W, Kochhar A, Patrick J, Heinemann S (1987) Members of a nicotinic receptor gene family are expressed in different regions of the mammalian central nervous system. Cell 48:965–973.

Kellar KJ, Giblin BA, Lumpkin MD (1989) Regulation of brain cholinergic sites by nicotine. Prog Brain Res 79:209–216.

Lee JJ, Costlow NA (1987) A molecular titration assay to measure transcript prevalence levels. Methods Enzymol 152:633–649.

Lindstrom J, Schoepfer R, Conroy WG, Whiting P (1990) Structural and functional heterogeneity of nicotinic receptors. In: The biology of nicotine dependence. CIBA Found Symp 152:23–52.

Lowry OH, Rosebrough NH, Farr AC, Randall RJ (1951) Protein measurement with the Folin phenol reagent. J Biol Chem 193:265–275.

Luetje CW, Patrick J, Seguela P (1990) Nicotine receptors in mammalian brain. FASEB J 4:2753–2760.

Marks MJ, Collins AC (1982) Characterization of nicotine binding in mouse brain and comparison with the binding of alpha-bungarotoxin and quiliculidinyl benzilate. Mol Pharmacol 22:554–564.

Marks MJ, Burch JB, Collins AC (1983) Effects of chronic nicotine infusion on tolerance development and cholinergic receptors. J Pharmacol Exp Ther 226:806–816.

Marks MJ, Stitzel JA, Collins AC (1985) Time course study of the effects of chronic nicotine infusion on drug response and brain receptors. J Pharmacol Exp Ther 235:619–628.

Marks MJ, Stitzel JA, Collins AC (1986a) Dose–response analysis of nicotine tolerance and receptor changes in two inbred mouse strains. J Pharmacol Exp Ther 239:358–364.

Marks MJ, Stitzel JA, Romm E, Wehner JM, Collins AC (1986b) Nicotinic binding sites in rat and mouse brain: comparison of acetylcholine, nicotine and alpha-bungarotoxin. Mol Pharmacol 30:427–436.

Marks MJ, Stitzel JA, Collins AC (1989) Genetic influences on nicotine responses. Pharmacol Biochem Behav 33:667–678.

Neve KA, Neve RL, Fidel S, Janowsky A, Higgins GA (1991) Increased abundance of alternatively spliced forms of D2 dopamine receptor mRNA after denervation. Proc Natl Acad Sci USA 88:2802–2806.

Papke RL, Boulter J, Patrick J, Heinemann S (1989) Single channel currents of rat neuronal nicotinic acetylcholine receptors expressed in *Xenopus* oocytes. Neuron 3:589–596.

Pauly JR, Stitzel JA, Marks MJ, Collins AC (1989) An autoradiographic analysis of cholinergic receptors in mouse brain. Brain Res Bull 22:453–459.

Pauly JR, Marks MJ, Gross SD, Collins AC (1991) An autoradiographic analysis of cholinergic receptors in mouse brain after chronic nicotine treatment. J Pharmacol Exp Ther 258:1127–1136.

Romano C, Goldstein AM (1980) Stereospecific nicotine receptors in rat brain. Science 210:647–649.

Schoepfer R, Conroy WG, Whiting P, Gore M, Lindstrom J (1990) Brain alpha-bungarotoxin binding protein cDNAs and MAbs reveal subtypes of this branch of ligand-gated ion channel gene superfamily. Neuron 5:35–48.

Schwartz RC, Kellar KJ (1983) Nicotinic cholinergic receptor binding sites in the brain: regulation *in vivo*. Science 220:214–216.

Senba E, Simmons DM, Wada E, Wada K, Swanson LW (1990) RNA levels of neuronal nicotinic acetylcholine receptor subunits are differentially regulated in axotomized facial motoneurons: an *in situ* hybridization study. Mol Brain Res 8:349–353.

Simmons DM, Arriza JL, Swanson LW (1989) A complete protocol for *in situ* hybridization of messenger RNAs in brain and other tissues with radiolabeled single-stranded RNA probes. J Histotechnol 12: 169–181.

Surgeon General (U.S. Department of Health and Human Services) (1988) The health consequences of smoking: nicotine addiction. A report of the Surgeon General. DHHS publication number (CDC) 88-8406. Rockville, MD: Public Health Service Office on Smoking and Health.

Swanson LW, Simmons DM, Whiting PW, Lindstrom J (1987) Immunohistochemical localization of neuronal nicotinic receptors in rodent central nervous system. J Neurosci 7:3334–3342.

van Tol HHM, Riva M, Civelli O, Creese I (1990) Lack of effect of chronic dopamine receptor blockade on D_2 dopamine receptor mRNA level. Neurosci Lett 111:303–308.

Wada E, Wada K, Boulter J, Deneris E, Heinemann S, Patrick J, Swanson LW (1989) Distribution of $\alpha 2$, $\alpha 3$, $\alpha 4$ and $\beta 2$ neuronal nicotinic receptor subunit mRNAs in the central nervous system: a hybridization histochemical study in the rat. J Comp Neurol 284:314–335.

Wada K, Ballivet M, Boulter J, Connolly J, Wada E, Deneris ES, Swanson LW, Heinemann S, Patrick J (1988) Functional expression of a new pharmacological subtype of brain nicotinic acetylcholine receptor. Science 240:330–334.

Whiting P, Lindstrom J (1986) Pharmacological properties of immunoisolated neuronal nicotinic receptors. J Neurosci 6:3061–3069.

Whiting P, Esch F, Shimasaki S, Lindstrom J (1987) Neuronal nicotinic acetylcholine receptor β-subunit is coded for by cDNA for $\alpha 4$. FEBS Lett 219:459–463.

Whiting P, Schoepfer R, Lindstrom J, Priestley T (1991) Structural and pharmacological characterization of the major brain nicotinic acetylcholine receptor subtype stably expressed in mouse fibroblasts. Mol Pharmacol 40:463–472.

Xu S, Monsma FJ, Sibley DR, Creese I (1992) Regulation of D_{1A} and D_2 dopamine receptor mRNA during ontogenesis, lesion and chronic antagonist treatment. Life Sci 50:383–396.